

Review Article

Toward Small-Scale Wind Energy Harvesting: Design, Enhancement, Performance Comparison, and Applicability

Liya Zhao and Yaowen Yang

Nanyang Technological University, 50 Nanyang Avenue, Singapore 639798

Correspondence should be addressed to Yaowen Yang; cywyang@ntu.edu.sg

Received 8 September 2016; Accepted 15 December 2016; Published 21 March 2017

Academic Editor: Mickaël Lallart

Copyright © 2017 Liya Zhao and Yaowen Yang. This is an open access article distributed under the Creative Commons Attribution License, which permits unrestricted use, distribution, and reproduction in any medium, provided the original work is properly cited.

The concept of harvesting ambient energy as an alternative power supply for electronic systems like remote sensors to avoid replacement of depleted batteries has been enthusiastically investigated over the past few years. Wind energy is a potential power source which is ubiquitous in both indoor and outdoor environments. The increasing research interests have resulted in numerous techniques on small-scale wind energy harvesting, and a rigorous and quantitative comparison is necessary to provide the academic community a guideline. This paper reviews the recent advances on various wind power harvesting techniques ranging between cm-scaled wind turbines and windmills, harvesters based on aeroelasticities, and those based on turbulence and other types of working principles, mainly from a quantitative perspective. The merits, weaknesses, and applicability of different prototypes are discussed in detail. Also, efficiency enhancing methods are summarized from two aspects, that is, structural modification aspect and interface circuit improvement aspect. Studies on integrating wind energy harvesters with wireless sensors for potential practical uses are also reviewed. The purpose of this paper is to provide useful guidance to researchers from various disciplines interested in small-scale wind energy harvesting and help them build a quantitative understanding of this technique.

1. Introduction

Studies on harvesting power from ambient energy sources have flourished in the past few years, with an ultimate objective to remove the reliance of low-power electronic devices on electrochemical batteries as well as the associated requirement of periodic replacement and maintenance. Various energy sources are available surrounding the electronic system, like solar, wind, thermal energy, mechanical vibration, and human activities. Among them, wind energy is ubiquitous and exists almost everywhere in our daily life, such as the flow in indoor heating and ventilation air conditioning systems and natural wind in outdoor spaces. It can serve as an alternative power supply to implement self-powered electronic systems like self-powered wireless sensor networks (WSNs). When a specific structure is subjected to wind flows, limit cycle oscillations will occur due to the fluid-structure interaction. The vibration strain energy can be beneficially transferred into electricity using various conversion mechanisms, such as electrostatic [1, 2], electromagnetic [3],

and piezoelectric conversions. Piezoelectric conversion has attracted rapidly growing interests due to the high power density and ease of integration with microsystems [1, 4–13].

Recently, the field of small-scale wind energy harvesting has experienced dramatic growth [14–21]. Researchers have reported studies on harnessing wind power using miniaturized windmills (e.g., [22]) or making use of aeroelastic instabilities such as vortex-induced vibration (VIV) (e.g., [23]), galloping (e.g., [24, 25]), aeroelastic flutter (e.g., [26]), and wake galloping (e.g., [27]). Turbulence-induced vibration has also been utilized for wind power extraction (e.g., [28]). Numerous techniques have emerged due to the growing research enthusiasm; therefore, a rigorous and quantitative comparison and review are necessary to provide the academic community a guideline. This paper focuses on a comprehensive comparison of various small-scale wind energy harvesting techniques, including cm-scaled wind turbines and windmills and harvesters based on aeroelasticities and turbulences as well as other types of working principles. In contrast to prior surveys [20, 21, 29–31], the emphasis of

this paper is laid on the quantitative comparison between the various fabricated prototypes in the literature regarding their dimensions, cut-in wind speeds, cut-out wind speeds, peak power values as well as power densities, and so forth, based on which merits, weaknesses, and applicability of different designs are discussed in detail. The main findings are summarized in Tables 1-2 and 4-8. Moreover, besides the technique comparison, enhancing methods of power extraction efficiency are reviewed and discussed from two aspects, that is, structural modification aspect and interface circuit improvement aspect. In addition, review is conducted on studies about integrating wind energy harvesters with wireless sensors for practical engineering applications. This paper aims to help researchers from various disciplines gain quantitative understanding of small-scale wind energy harvesting techniques and provide useful guidance to those who want to develop and improve the efficiency of a wind energy harvester.

2. Designs of Aeroelastic Piezoelectric Energy Harvesters

Many designs of small-scale wind energy harvesters have been reported in the literature, including those in the form of small-scale windmills and turbines and those based on the aeroelastic instabilities, like VIV, galloping, flutter, wake-induced oscillation, and TIV. In this section, performances of the recent small-scale wind energy harvester designs will be reviewed and compared.

2.1. Small-Scale Windmill and Wind Turbine. Rancourt et al. [35] investigated the performance of power generation of a centimeter-scale windmill. Power was generated using electromagnetic transduction mechanism. Three prototypes of propellers were tested in the wind tunnel, which were all 4.2 cm in diameter with four blades of different pitch angles. The experimental results showed that the “Schmitz theory,” which was developed for large scale wind turbine to determine the optimal tip speed ratio for maximum turbine efficiency (i.e., kinetic power extracted from the wind over the available kinetic flow energy for the area covered by the disk of the propeller), was also valid for small-scale wind turbines. However, the power generation efficiency (electrical power output over the available kinetic flow energy for the area covered by the disk of the propeller) at low wind speed decreased sharply due to the friction in the generator and the internal electric resistance. At a high wind speed of 11.8 m/s a large power of 130 mW was achieved, corresponding to a power generation efficiency of 9.5%, while a lower power of 2.4 mW was obtained at 5.5 m/s with a decreased efficiency of 1.85%.

Bansal et al. [77] and Howey et al. [36] tested a miniature electromagnetic wind turbine in cm-scale claimed to be the smallest turbine-based energy harvester reported to date, with a rotor diameter of 2 cm and outer diameter of 3.2 cm. The turbine [36] consisted of two rotating magnetic rings mounted on the rim of the rotor and fixed stator coil sandwiched between the magnetic rings. Wind tunnel experiment found that the cut-in wind speed was 3 m/s, below which the turbine could not operate. The test was run up to 10 m/s,

and a power of 80 μ W to 4.3 mW was achieved. Compared to the device of Rancourt et al. [35] at a low wind speed of 5.5 m/s, similar power generation efficiency was obtained, that is, 1.35% for 5 m/s and 1.52% for 6 m/s. It was noted that, at wind speeds lower than 7 m/s, the generated power was limited by bearing loss while, at wind speeds higher than 7 m/s, power output was limited by resistive generator loss. Future designs of miniature turbines aimed to harvest energy from low speed flows should pay attention to these two issues.

Both studies of Rancourt et al. [35] and Howey et al. [36] show that the major challenge of miniature electromagnetic windmill lies in the greatly decreased power generation efficiency in slow flows. Of course, if a more sophisticated small-scale wind turbine can be established incorporating optimized shape of airfoil and proper design of diffuser, the output power can be significantly increased [78, 79]. It was reported by Kishore et al. [79] that a properly designed small-scale wind energy portable turbine (SWEPT) with a diameter of 39.4 cm can generate a power-up to 830 mW at a wind speed of 5 m/s. Yet this size of the turbine is much larger than those of the small-scale harvesters mentioned above, which are mainly smaller than or in the order of 10 cm.

Recently small-scale windmills using piezoelectric transduction have shown great potential in efficiently harvesting low speed flow energy. The rotation of the windmill shaft under wind flows is transferred to oscillatory motion of the piezoelectric transducer. The mechanical transfer is sometimes achieved by direct impact between the piezoelectric cantilever and the cam or blade, with a working principle similar to that of a mechanical stopper [80]; some other times it is achieved through magnetic interaction where no contact impact is required.

Priya et al. [22] proposed a piezoelectric windmill to harvest energy from low speed wind flows. Twelve piezoelectric bimorphs were arranged in a circular array around the circumference of the center shaft of the windmill. Twelve rubber stoppers were connected to the shaft, each of which was in contact with one of the bimorphs. The shaft connected via a cam to a rotating fan was rotated via the camshaft mechanism. When the shaft rotated, the stoppers caused the back and forth movements of the bimorph transducers, generating electrical energy via direct piezoelectric effect. The voltage was measured across a 4.6 k Ω load at an oscillatory frequency of 4.2 Hz. Experimentally, a standard circuit was employed and a power of 10.2 mW after rectification was obtained at 6 Hz and 4.6 k Ω . It was found that power was increased with the prestress level and the number of bimorphs, which yet also resulted in increased difficulty in the fan rotation thus causing an increased cut-in wind speed.

In a subsequent work, Priya [37] presented a theoretical model based on bending beam theory of bimorphs and equivalent circuit of capacitor to predict the output power of the above-mentioned piezoelectric windmill. Ten bimorphs were used in the experiment. A cut-in wind speed of 4.7 mph and a cut-out wind speed of 12 mph (above which damage of structure will occur) were measured. A maximum power of 7.5 mW was obtained after rectification at 10 mph across a load of 6.7 k Ω . A linear relationship was given between the saturated frequency (final constant operating frequency at a

TABLE I: Summary of various small-scale windmills and wind turbines.

Author	Transduction	Mechanical transfer	Cut-in wind speed (m/s)	Cut-out wind speed (m/s)	Maximum power (mW)	Wind speed at max power (m/s)	Dimensions	Power density per swept area (mW/cm ²)	Advantages/disadvantages
Rancourt et al. [35]	Electromagnetic	—	—	—	130	11.8	4.2 cm in dia.	9.38	(i) High power generation efficiency at high wind speed. (ii) At low wind speed, efficiency decreased sharply due to the friction in the generator and the internal electric resistance
Howey et al. [36]	Electromagnetic	—	3	—	4.3	10	3.2 cm in dia.	0.535	(i) Bearing loss and resistive generator loss limits the miniaturization of the turbine
Priya et al. [22]	Piezoelectric	Contact via mechanical stopper	—	—	10.2	—	12 bimorphs in a circular array, each of $6 \times 2 \times 0.05$ cm ³	0.0902	(i) Proves the feasibility of efficiently harvesting low speed wind energy using piezoelectric materials.
Priya [37]	Piezoelectric	Contact via mechanical stopper	2.1	5.4	7.5	4.5	10 bimorphs in a circular array, each of $6 \times 2 \times 0.06$ cm ³	0.0663	(ii) Bimorphs are not vibrating in phase so the output has to be individually processed
Chen et al. [38]	Piezoelectric	Contact via mechanical stopper	2.1	6.2	1.2	5.4	$5.08 \times 11.6 \times 7.62$ cm ³	0.0134	(i) Easy to fabricate. (ii) Space efficient with a rectangular-array arrangement of transducers. (iii) Combined circuit can be used because all the bimorphs are vibrating in phase. (iv) Power was much lower compared to the circular windmill
Myers et al. [39]	Piezoelectric	Contact via mechanical stopper	2.4	—	5	4.5	$7.62 \times 10.16 \times 12.70$ cm ³	0.0388	(i) Captured wind energy is increased by employing three fan blades
Bressers et al. [40]	Piezoelectric	Contact-less via magnetic interaction	0.9	—	1.2	4.0	$16.51 \times 16.51 \times 22.86$ cm ³ ;	3.18×10^{-3}	(i) Minimizing the frictional loss by avoiding direct mechanical contact. (ii) Prolonging the fatigue life of piezoelectric elements.
Karami et al. [41]	Piezoelectric	Contact-less via magnetic interaction	2	—	4	10	$8 \times 8 \times 17.5$ cm ³	0.0286	(iii) Lowering down the cut-in wind speed (i) Introducing nonlinearity into the harvester. (ii) Utilizing both nonlinear parametric excitation and ordinary excitation and helping to achieve low cut-in wind speed, high output power, and large operational range of wind speed

TABLE 2: Summary of various VIV energy harvester devices¹.

Author	Transduction	Bluff body shape	Wind speed at		Cut-in wind speed (m/s)	Cut-out wind speed (m/s)	Maximum power (mW)	max power (lock-in) (m/s)	Dimensions	Power density per volume (mW/cm ³) ^{±1}	Advantages/disadvantages and other information
Allen and Smits [42] (in water)	Piezoelectric	Plate	0.05 (water speed)	0.8 (water speed)	—	—	—	—	Bluff body, frontal dimension: 5.05 cm & 3.81 cm. Eel membrane, length: 45.7 cm & 7.6 cm PVDF eel: 24 cm × 7.6 cm × 150 μm		(i) Investigated and confirmed the feasibility of harvesting fluid energy via VIV. (ii) Determines that optimal performance occurs at resonance condition
Taylor et al. [43] (in water)	Piezoelectric	Plate	—	—	3 V (peak voltage)	0.5 (water speed)	—	—		1.10 (V/cm ³)	(i) The use of windward bluff body and mass on the free end of the flapping piezoelement can enhance energy conversion. (ii) Experimentally proves the use of quasi-resonant rectifier can increase the efficiency by a factor of 2.3 compared to a standard full-wave rectifier. (iii) Theoretically confirms the use of AFC/MFC can increase the efficiency by a factor of 25 compared to PVDF
Robbins et al. [44]	Piezoelectric	Cylinder	—	—	7.8	6.7	—	—	Flapping PVDF membrane: 25.4 cm × 17.78 cm × 457.2 μm	0.378	(i) The use of piezoelectric bimorph cantilever ensures only the first mode deformation to guarantee no charge cancellation on the surface. (ii) Theoretically proposes the optimal geometry of $L/D = 2.125$. (iii) Adjacent cantilevers arrangement enhances output power
Pobering and Schwesinger [45]	Piezoelectric	Polygon	4.5	45	0.108	45	—	—	Bluff body frontal dimension: 1.035 cm. Three identical cantilevers: $1.4 \times 1.18 \times 0.035 \text{ cm}^3$	0.0817	(i) Experimentally validates the optimal geometry of $L/D = 2.125$. (ii) Use of stapled piezoelectric layers enhance output power. (iii) Adjacent cantilevers arrangement can further lower the cut-in wind speed down to 8 m/s
Pobering et al. [46]	Piezoelectric	D-shape	15	—	1	40	—	—	Bluff body frontal dimension: 1.035 cm. Nine identical cantilevers (Series I): $2.2 \times 1.18 \times 0.035 \text{ cm}^3$	0.164	(i) The driving mechanism of the beam's oscillation was discovered via CFD as the combined effect of the overpressure resulting from the stagnation region and the suction of the core of another vortex on the opposite side. (ii) The optimal position of the upstream tip of the cantilever was found to along the centerline and at a distance of $x/D = 2$. (iii) Nonattachment of bluff body and cantilever results in very low output power
Akaydin et al. [47]; Akaydin et al. [48]	Piezoelectric	Cylinder	—	—	0.004	723	—	—	Bluff body: 3 cm in dia., 1.2 m in length. Cantilever: $3 \times 1.6 \times 0.02 \text{ cm}^3$	4.72×10^{-6}	

TABLE 2: Continued.

Author	Transduction	Bluff body shape	Cut-in wind speed (m/s)	Cut-out wind speed (m/s)	Maximum power (mW)	Wind speed at max power (lock-in) (m/s)	Dimensions	Power density per volume (mW/cm ³) ^{*1}	Advantages/disadvantages and other information
Akaydin et al. [23]	Piezoelectric	Cylinder	—	—	0.1	1.192	Bluff body: 1.98 cm in dia., 20.3 cm in length. Cantilever: 26.7 × 3.25 × 0.0635 cm ³	1.47 × 10 ⁻³	(i) Attachment of the cylinder on the cantilever tip and use of PZT instead of PVDF greatly enhanced the output power. (ii) Attachment of the cylinder on the cantilever tip reduces the resonance wind speed for maximum power
Weinstein et al. [49]	Piezoelectric	Cylinder	2	5 (5.5)	5	5.5	Bluff body: 2.5 cm in dia., 11 cm in length. Cantilever: 2.86 × 0.63 × 0.25 cm ³ Whole plane size: 22.5 × 11 cm ²	0.0918	(i) Operational wind speed range is broadened, because the harvester's resonance frequency and its resonance wind speed can be tuned by adjusting the position of the added weight. (ii) Tuning mechanism is not automatic
Gao et al. [50]	Piezoelectric	Cylinder	3.1	—	0.03	5 (turbulent flow speed)	Bluff body: 2.91 cm in dia., 3.6 cm in length. Cantilever: 3.1 × 1.0 × 0.0202 cm ³	1.25 × 10 ⁻³	(i) Turbulent flow results in higher output power of harvester than laminar flow. (ii) Turbulence excitation is claimed to be the dominant driving mechanism of the harvester; vortex shedding excitation in the lock-in region gives add-on contribution. (iii) Cantilever and cylinder are in parallel
Wang and Ko [51]	Piezoelectric	N.A.	—	—	2 × 10 ⁻⁴	—	PVDF film: 2.5 × 1.3 × 0.0205 cm ³ Bluff body: 4.25 mm & 1 mm in bases, 1.63 mm in height. Magnet: 0.8 × 0.8 × 1 cm ³	3.00 × 10 ⁻³	(i) Can be easily deployed in the pipelines, tire cavities, or machinery by installing a diaphragm on the wall. (ii) Output power is relatively low compared to other devices.
Wang et al. [52]	Electromagnetic	Trapezoidal	—	—	1.77 × 10 ⁻³	1.38 (water speed)	Coil: 2 cm in dia., 0.2 cm in thickness Two identical bluff bodies: 0.425 cm in base length, 0.218 cm in altitude. PVDF film: 2.5 × 1.3 × 0.0205 cm ³	1.33 × 10 ⁻³	(iii) Methods of enhancing power are proposed, for example, optimizing the blockage ratio, adjusting the diaphragm position, and using material with high piezoelectric constants
Tam Nguyen et al. [53]	Piezoelectric	Triangle	—	—	5.9 × 10 ⁻⁷	20.7		3.70 × 10 ⁻⁶	

¹If more than one sized prototypes were investigated in the reference, the information of dimension and critical wind speeds listed in the table corresponds to the one giving maximum output power.

^{*1}The device volume is approximated without considering the piezoelectric element volume, thus the power density calculated is the conservative estimates showing the upper bound.

constant wind speed) of the windmill and the wind speed as $f \text{ (Hz)} = -0.93 + 1.29U$, which well captured the experimental observation that the frequency linearly increased with the wind speed. Also, it was found that the generated power almost linearly increased with the frequency. It was suggested that the piezoelectric windmill could be a feasible power supply for wireless sensors.

Chen et al. [38] investigated the performance of wind energy harvester with similar working principle to that of the above piezoelectric windmills, but with a rectangular arrangement of piezoelectric transducers. Twelve bimorph transducers were arranged in six rows and two columns, with a gap of 6 mm between each other. A cylindrical rod in between the two columns was connected via a camshaft mechanism to a rotating fan, which caused the up and down movement of the rod. Subsequently, the six hooks on the rod induced back and forth oscillations of the transducers from which electrical energy could be generated. The variation of power with wind speed from experiment was similar to that of Priya [37]. With a load of 1.7 k Ω , a cut-in wind speed of 4.7 mph and a cut-out wind speed of 14 mph were measured, with a maximum power of 1.2 mW obtained at 12 mph. Compared to the windmill, this prototype is easy to fabricate and is space efficient with a rectangular-array arrangement of transducers; also, since all the bimorphs are vibrating in phase, combined circuit can be used eliminating the trouble of using individual processing circuit required in the circular windmill, as summarized by Myers et al. [39]. Yet the power was much lower compared to the circular windmill. To solve this issue, Myers et al. [39] proposed an optimized rectangular piezoelectric windmill to enhance power output by employing three fan blades to enlarge the covered flow surface and to increase the captured wind energy. The number of piezoelectric transducers was also increased, with two rows containing nine transducers in each row. It was measured that, with a small sized prototype of $3 \times 4 \times 5 \text{ inch}^3$ ($7.62 \times 10.16 \times 12.70 \text{ cm}^3$), an enhanced power of the order of 5 mW was obtained at 10 mph. It should be noted that, for all the above-mentioned piezoelectric windmills, the same piezoelectric transducers were used, that is, APC 855 with dimensions of a single piece of $60 \times 20 \times 0.6 \text{ mm}^3$.

For the above-mentioned impact-driven windmills, a challenging issue exists that the frequent impacts not only dissipate some kinetic energy but also cause fatigue problems of the piezoelectric cantilevers and induce mechanical damages. In order to overcome this shortcoming, some researchers have proposed windmills that do not require direct impacts but induce oscillations of the transducers through magnetic interactions.

Bressers et al. [40] proposed a design of piezoelectric wind turbine where the piezoelectric elements were “contact-less” actuated through magnetic interaction. A vertical axis wind turbine was connected to a disk, to which a series of alternating polarity magnets were attached. The magnets were also attached at the tips of the cantilevered transducers, which underwent harmonic oscillations through alternating attractive/repulsive magnetic force when the blades were rotating in wind flow. Measurement showed that with a two-blade and four-magnet rotor, the cut-in wind speed was

lowered down to 2 mph and a maximum power of around 1.2 mW was obtained at 9 mph.

Karami et al. [41] proposed a nonlinear piezoelectric wind turbine. A vertical axis turbine was placed on top of four vertical cantilevered piezoelectric transducers. Two arrangements of tangential configuration ($80 \times 80 \times 175 \text{ mm}^3$) and radial configuration ($75 \times 75 \times 165 \text{ mm}^3$) were considered. In both configurations, four tip magnets were embedded at the tips of the transducers, while five magnets were attached to the bottom of the rotating disk that was fixed to the blades. Different from the device of Bressers et al. [40], nonlinearity was introduced to the transducers. The rotation of the blades induced the distance between the disk and tip magnets to continuously alter, making the transducer alternately undergo bistable and monostable dynamics. Therefore, the transducer was both directly and parametrically excited. For the tangential configuration, with a magnetic gap of 25 mm and a load of 247 k Ω , the cut-in wind speed was measured to be 2 m/s, and a maximum power of 4 mW at 10 m/s was obtained, while, for the radial configuration, the output power was one order of magnitude less than that from the tangential design. It was explained that the direct excitation in the radial configuration was not as significant as that in the tangential configuration. It was concluded that the nonlinear parametric excitation and ordinary excitation mechanisms can result in several advantages, including the low cut-in wind speed, high output power, and large operational range of wind speed.

Miniaturized windmills or wind turbines can generate a significant amount of power. Yet the biggest concern is that the rotary components are not desired for long-term use of such small sized devices. A summary of the various windmills and miniaturized turbines reviewed is presented in Table 1. Their merits or limitations and other information that the authors feel useful are also given in the table. For the present table and the following ones (Tables 2 and 4–8), power density per swept area/volume is calculated by dividing the maximum output power by the frontal area normal to the flow/device volume. Because the volume of some accessory components (e.g., the joints) and elements taking very small proportions of the whole volume (e.g., a short piezoelectric sheet attached to a long substrate cantilever) are ignored, the power density values should be considered the estimated upper bound for comparison purpose only.

2.2. Energy Harvesters Based on Vortex-Induced Vibrations.

The concept of using VIV to harvest energy was first investigated in flowing water instead of wind. Allen and Smits [42] proposed an “energy harvesting eel” to harvest flowing water energy. The unit consisted of a fixed flat plate as a bluff body with a piezoelectric membrane placed in the wake. The membrane was set free in the downstream. Alternating vortices were shedded on either side of the bluff body, resulting in pressure differential thus forcing the membrane to oscillate with a movement similar to that of a natural eel swimming. Particle image velocimetry (PIV) experiment was conducted to investigate the vorticity pattern formed behind the bluff body. Four prototypes were tested in a recirculating water channel with different types of material and dimensions

of the membrane and various Reynolds number. It was found that lock-in phenomenon occurred to the membranes when they oscillated at the same frequency as the undisturbed wake behind the bluff body. The frequency responses of the membrane were found to be independent of the length of the membrane but significantly sensitive to the bluff body size. Electrical response (i.e., voltage or power) was not measured in this study.

Taylor et al. [43] proposed a similar “eel” harvester to harvest energy from flowing water like in the estuary or even in the open ocean. A prototype of 9.5" length, 3" width and 150 μm thickness was fabricated with the commercial piezoelectric polymer PVDF, totally consisting of 8 segments. The prototype was tested in a flow tank and data on each segment were acquired separately. A peak voltage around 3 V was measured for the segment near the head bluff body at a flow speed of 0.5 m/s. Measurements also showed that, from head to tail, distortion in the voltage output increased while voltage magnitude decreased. The maximum power was achieved when the flapping frequency matched the vortex shedding frequency. It was pointed out that an optimum central layer and active layer thickness deserve further design efforts to obtain the optimum bending stiffness and thus the maximum strain.

Robbins et al. [44] proposed several methods to improve the power extraction efficiency of an energy harvester with flexible piezoelectric material. It was shown experimentally that the efficiency could be enhanced by using windward bluff body and adding mass to the free end of the flapping piezoelement. Analytically, it was shown that the use of stronger-coupling flexible piezoelectric materials such as AFCs (active fiber composites) and MFCs (macrofiber composite) could improve the efficiency by a factor of 25. Moreover, both experiment and analysis showed that using the quasi-resonant rectifier to extract electrical energy from piezoelement instead of standard full-wave rectifier could increase the efficiency by a factor of 2.3.

Pobering and Schwesinger [45] implemented a VIV energy harvester similar to the energy harvesting eel in both the air and water flow. It was roughly determined that available energy densities in flowing media are in the range of 256 W/m² in air at a wind speed of 10 m/s and 1600 kW/m² in water at a flow speed of 2 m/s, respectively. Behind the fixed bluff body, a piezoelectric bimorph cantilever was attached instead of flexible membrane or polymer, in such a way that the cantilever would only deform in the first vibration mode, unlike in the case of the membrane or polymer where undulating waves were generated along the length. With a simple analytical model, the optimal ratio of the cantilever length L over the frontal dimension D of the windward bluff body was calculated to be $L/D = 2.125$. Three identical prototypes were fabricated and tested in a row with a cantilever length of 14 mm, width of 11.8 mm, thickness of 0.35 mm, and bluff body frontal dimension of 10.35 mm. The wind speed giving the peak power varied for the three prototypes depending on their positions. A highest deflection of 51 μm was obtained at a wind speed of 40 m/s on the second cantilever. A peak voltage of 0.8 V with a load resistance of 1 M Ω and a peak power of 0.108 mW with a matched load

resistance of 1.2 k Ω were measured at 45 m/s. Measurements in the water were not reported, but it was predicted that lower water flow speed would lead to comparable high power since the energy density in water was around 1000 times higher than that in air. It was concluded that adjacent cantilevers had strong influences on each other which enhanced the deflection and output power.

In a subsequent study, Pobering et al. [46] conducted more tests in both air and water. Comparison of the wind tunnel experimental results between two series confirmed the analytical prediction of the optimal geometrical relationship $L/D = 2.125$. It was also found that the cantilevers in a row were able to synchronously oscillate in flowing media with high density like water. With a peak power of 0.055 mW obtained from a single piezoelectric layer at 40 m/s, a total power output of around 1 mW can be approximated for a series of 9 cantilevers. It was concluded that the power of the proposed harvesting system was sufficient to power sensors logical circuits and wireless data transmission circuits.

However, among the above studies on VIV based energy harvesters, no one has investigated the effect of electromechanical coupling on the electrical output or its backward coupling effect on the aeroelastic response. Akaydin et al. [47] were among the very first to consider the three-way coupling effects, that is, the mutual coupling behaviors between the aerodynamics, structural vibration, and electrical response. In their study, a new type of energy harvester was proposed to harness flow energy based on the vortex shedding phenomenon. A piezoelectric cantilever was put behind a windward cylinder which was fixed as a bluff body. The downstream end of the cantilever was fixed. The cantilever oscillated in the fully turbulent vortex street formed at high Reynolds number of 14842. Although the harvester was claimed to be designed for harnessing energy from highly unsteady fluid flows, if we consider the windward cylinder as a part of the energy harvester the flow in front of the cylinder was smooth and steady as they were placed together in a smooth-flow-generating wind tunnel. Therefore, we review this design in the section of “energy harvesters based on vortex-induced vibrations.” In this study, performance of the piezoelectric cantilever inside a turbulent boundary layer was also reported, which we will introduce in the section of “energy harvesters based on turbulent induced vibration.” Experimentally, with a 30 mm \times 16 mm \times 0.2 mm cantilever with a piezoelectric layer of PVDF attached on the top surface and with a cylinder of 30 mm in diameter and 1.2 m in length fixed in the windward direction, a peak power of 4 μW was measured with a load of 100 k Ω at a wind speed of 7.23 m/s, which produced a vortex shedding frequency close to the beam’s resonance frequency around 48.5 Hz. Simulations based on CFD were conducted to solve the two-dimensional N-S (Navier-Stokes) equations to obtain the aerodynamic pressure, which was substituted into a 1DOF electromechanical model to calculate the voltage output. The electromechanical coupling was assumed to be weak and the backward coupling effect of the voltage generation on the mechanical displacement response was reasonably ignored. An explanation of the driving mechanism of the beam’s oscillation was tried to be deduced from the simulation

results. The induced flow ahead of the vortex impinges on the beam, and the overpressure resulting from the stagnation region bends the beam; at the same time, on the opposite side, the core of another vortex applies suction, driving the beam in the same direction. The mechanism was further confirmed in a subsequent study with more simulations [48]. It was found experimentally that the face-on configuration where the beam was parallel to the upstream flow is the best orientation for the beam.

In a subsequent study, Akaydin et al. [23] proposed a new self-excited VIV energy harvester to improve the output power. The cylinder was, different from the previous cases, attached to the free end of an aluminum cantilever with PZT covering the end area. Periodic oscillations occurred in the direction normal to the wind flow due to the vortex shedding. A peak power of around 0.1 mW of nonrectified power was obtained at a much lower wind speed of 1.192 m/s with a matched load of 2.46 M Ω . Compared to the previous design, the aeroelastic efficiency (i.e., efficiency of converting the flow energy into mechanical energy) was increased from 0.032% to 2.8% and the electromechanical efficiency (i.e., efficiency of converting the mechanical energy into electrical energy) was increased from 11% to 26%. It was concluded that the modified configuration of the attachment of the cylinder on the cantilever tip and the employment of PZT instead of PVDF greatly enhanced the power generation.

In order to overcome the narrow operating range of VIV-based harvesters, Weinstein et al. [49] proposed an energy harvester with resonance tuning capabilities. The piezoelectric cantilever was placed behind a cylinder bluff body and attached with an aerodynamic fin at the tip. Small weights were placed along the fin. Manually adjustment of the weights positions could tune the resonant frequencies of the harvester, making it able to operate at resonance for wind velocities from 2 to 5 m/s. A peak power of nearly 5 mW was obtained at a wind speed of around 5.5 m/s. But the limitation is that this tuning mechanism is not automatic; thus the wind velocity needs to be always stable and the exact wind velocity should be known before the installation of this harvester.

Different from the aforementioned studies which investigated the performance of the fabricated VIV energy harvester prototypes based on experiments or numerical simulations, Barrero-Gil et al. [81] attempted to theoretically evaluate the effects of the governing parameters on the power extraction efficiency. The effects of the mass ratio m^* (i.e., the ratio of the mean density of a cylinder bluff body to the density of the surrounding fluid), the mechanical damping ζ , and the Reynolds number were investigated with a 1DOF model where fluid forces were introduced from previously published experimental data from forced vibration tests. There was no specific energy harvester design proposed. It was shown that the efficiency was greatly influenced by the mass-damping parameter $m^*\zeta$, and there existed an optimal $m^*\zeta$ for peak efficiency at a specific Reynolds number. The range of reduced wind speeds with significant efficiency was found to be mainly governed by m^* . Also, it was found that high efficiency could be achieved for high Reynolds numbers.

Abdelkefi and his coworkers [82, 83] theoretically analyzed the influences of several parameters on the mechanical and electrical responses of a VIV harvester. A flexibly supported rigid cylinder was considered with a piezoelectric transducer attached to the transverse degree of freedom. The vortex shedding lift force was expressed by a van der Pol equation. Based on the lumped parameter model, Abdelkefi et al. [82] found that increasing the load resistance shifted the onset of synchronization to higher wind speeds. A hardening behavior and hysteresis were observed in the displacement, voltage, and power responses due to the cubic nonlinearity in the lift coefficient. In a subsequent study of Mehmood et al. [83], the aerodynamic loads due to vortex shedding were obtained using CFD simulations and were subsequently coupled with the electromechanical model to predict the electrical output. It was found that the region of wind speeds at synchronization was slightly widened when the load resistance increased. An optimum value of load resistance for maximum power output was determined to correspond to the load value with minimum displacement of the cylinder.

Gao et al. [50] proposed another configuration of harvester consisting of a piezoelectric cantilever with a cross-flow cylinder attached to its free end, of which the long axes were arranged in parallel. Prototypes were constructed and tested in both laminar flows generated by a wind tunnel and turbulent flows generated by an electric fan. Experimentally, it was found that the power output increased with the wind speed and cylinder diameter. Higher voltage and power were generated in the turbulent flow than in the laminar flow. It was concluded that turbulence excitation was the dominant driving mechanism of the harvester, with additional contribution from vortex shedding excitation in the lock-in region. With a piezoelectric cantilever of $31 \times 10 \times 0.202 \text{ mm}^3$ and a cylinder with a length of 36 mm and a diameter of 29.1 mm, a peak power of 30 μW was measured at a wind speed of 5 m/s in the fan-generated turbulent flow.

Instead of directly using the impinges of shedded vortices on the piezoelectric membrane or cantilever to induce mechanical oscillations, Wang and his coworkers [51–53, 84] developed energy harvesters in the form of a flow channel with a flexible diaphragm. The diaphragm was driven into vibration by vortex shedding from a bluff body placed in the channel. Piezoelectric film or magnet and coil are connected to the diaphragm for energy transduction. Experimental results showed that an instantaneous output power of 0.2 μW was generated for the piezoelectric harvester under a pressure amplitude of 1.196 kPa and a pressure frequency of 26 Hz [51] and 1.77 μW for the electromagnetic harvester under 0.3 kPa and 62 Hz [52]. Subsequently, Tam Nguyen et al. [53] further investigated the effects of different bluff body configurations. Two bluff bodies were placed in the flow channel in a tandem arrangement to enhance the pressure fluctuation behind them. A prototype was assembled, with an embedded 0.2 mm thick polydimethylsiloxane (PDMS) diaphragm on top surface of the flow channel, two triangular bluff bodies with a base length of 4.25 mm, and an altitude of 2.18 mm inserted inside a PVDF film of 25 mm \times 13 mm \times 0.205 mm glued to the acrylic glue on top of the diaphragm.

An open-circuit voltage of 14 mV and an average power of 0.59 nW were measured with the prototype at a wind speed of 20.7 m/s. The power is relatively low as compared with other harvesters that have been reviewed. It was suggested that the power can be enhanced by optimizing the blockage ratio, adjusting the position of the flexible diaphragm, and using a piezoelectric material with higher piezoelectric constants. This harvester design was recommended to be deployed in the pipelines, tire cavities, or machinery by installing a diaphragm on the wall.

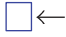

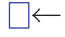
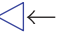
Current studies on energy harvesting from VIV also include the investigation of the interaction of a single and multiple vortices with a cantilever conducted by Goushcha et al. [85] as an extension of the work by Akaydin et al. [47, 48]. Particle image velocimetry was used to measure the flow field induced by each controllable vortex and quantify the pressure force on the beam to give a better understanding of the fluid-structure interactions. The two driving mechanisms of upstream flow impingement on one side of beam and suction of the vortex core on the opposite side [47, 48] and the importance of matching the frequency of appearance of vortices with the beam's resonance frequency were demonstrated clearly via the flow visualization.

The necessity of achieving the synchronization region for energy harvesting from VIV was also demonstrated by Wang et al. [86] through modeling with computational fluid dynamics. Recently, VIV has been employed for large-scale wind energy harvesting with the so-called Vortex Bladeless Wind Generator [87], which is capable of generating high output power in the order of kW or even MW. The size of this type of generator is tremendously increased as compared to other devices investigated here; for example, it can be a few tens of meters high. Table 2 compares the reported fabricated prototypes based on vortex-induced vibrations, with regard to the transduction mechanism, shape of bluff body, cut-in and cut-wind speed, peak power and power density, dimension, and their advantage, disadvantage, and applicability.

2.3. Energy Harvesters Based on Galloping. It is not until recently that the aeroelastic instability phenomenon of transverse galloping is employed to obtain structural vibrations for energy harvesting purpose. Due to the self-excited and self-limiting characteristics of galloping, it is a prospective energy source for energy harvesting. Moreover, compared to the VIV, galloping owns its advantages of large oscillation amplitude and the ability of oscillating in infinite range of wind speeds, which are preferable for energy harvesting.

Barrero-Gil et al. [88] theoretically analyzed the potential use of galloping to harvest energy using a 1DOF model. The harvesting system was modeled as a simple mass-spring-damper system. No specific energy harvester design was proposed. The aerodynamic force was formulated using a cubic polynomial based on the quasi-steady hypothesis. Theoretically, it was found that, in order to achieve a high efficiency, the bluff body should have a high aerodynamic coefficient A_1 and a low absolute value of A_3 (generally, $A_1 > 0$, $A_2 = 0$, and $A_3 < 0$). For the mechanical damping, it was determined that a low value of the mass-damper parameter

TABLE 3: Different cross-sections of bluff body in comparative study of Yang et al. [32].

Section shape				
Dimension $h \times d$ (mm)	40 × 40	40 × 60	40 × 26.7	40 (side) 40 (dia.)

$m^* \zeta$ should be used, where m is the distributed mass of the bluff body. Sorribes-Palmer and Sanz-Andres [89] continue the study by obtaining the aerodynamic coefficient curve $C_z(\alpha)$ directly from the experimental data instead of using a polynomial fitting. It was found that directly obtaining $C_z(\alpha)$ from experiment can avoid problems associated with polynomial fitting like wrong dynamic responses induced by inaccurate polynomials.

A galloping energy harvester consisting of two cantilever beams of $161 \times 38 \times 0.635 \text{ mm}^3$ and a prism with equilateral triangular cross-section of 40 mm in each side and 251 mm in length attached to the free ends was proposed by Sirohi and Mahadik [54]. A coupled electromechanical model was established based on the Rayleigh-Ritz method, and the aerodynamic model was based on the quasi-steady hypothesis. Due to the large size and high coupling coefficient of the piezoceramic sheets, a high peak power was achieved as more than 50 mW at a wind velocity of 11.6 mph (around 5.2 m/s) in the laminar flow condition. But an abrupt decrease in output power occurred at 13.6 mph, which was not in consistence with the galloping mechanism. The authors attributed this decrease to the large-scale turbulence in the wind tunnel.

Another galloping energy harvester using a tip body with D-shaped cross-section connected in parallel with a piezoelectric composite cantilever was developed by Sirohi and Mahadik [55], with a dimension of 30 mm in diameter and 235 mm in length for the tip body and $90 \times 38 \times 0.635 \text{ mm}^3$ for the cantilever. The wind flow was generated by an axial fan, which was associated with a highly turbulent profile. The measured voltage generated by the piezoelectric sheets showed that a stable limit cycle oscillation could be obtained for the steady state response. Also, the frequency of oscillation was found to be equal to the natural frequency of the cantilever. The power output was observed to continuously increase with the wind speed. A maximum power of 1.14 mW was obtained at a wind speed of 10.5 mph. The wide operational wind speed range is a great benefit of energy harvesters based on galloping.

A comparative study of different bluff body cross-sections for small-scale wind energy harvesting based on galloping was conducted by Zhao et al. [56] and Yang et al. [32]. Wind tunnel experiment was carried out with a prototype device consisting of a piezoelectric cantilever and a bluff body with various cross-section profiles. Square, rectangle, triangle, and D-shape were considered, as shown in Table 3. Figure 1 shows an example of the schematic and fabricated prototype of the galloping energy harvester with a square bluff body. Responses of power versus load resistance showed that there existed an optimal load value for maximum output power. Moreover, it was experimentally determined for the first time

TABLE 4: Summary of various galloping energy harvester devices.

Author	Transduction	Bluff body shape	Cut-in wind speed (m/s)	Cut-out wind speed (m/s)	Maximum power (mW)	Wind speed at max power (m/s)	Dimensions	Power density per volume (mW/cm ³)	Advantages/disadvantages and other information
Sirohi and Mahadik [54]	Piezoelectric	Triangle	3.6	6.1	50	5.2	Bluff body: 4 cm in side, 25.1 cm in length; cantilever: 16.1 × 3.8 × 0.0635 cm ³	0.281	(i) High peak power is achieved, with high electromechanical coupling. (ii) Validates the feasibility of predicting galloping energy harvester's response with quasi-steady hypothesis. (iii) Abrupt decrease in output power at 6.1 m/s is undesired.
Sirohi and Mahadik [55]	Piezoelectric	D-shape	2.5	—	1.14	4.7	Bluff body: 3 cm in dia., 23.5 cm in length; cantilever: 9 × 3.8 × 0.0635 cm ³	0.0134	(i) Output power continuously increases with wind speed, with no cut-out wind speed. (ii) Wide operational wind speed range. (iii) Requiring turbulent flow to function well, for example, flow from a rotating fan, because D-shape cannot self-oscillate in laminar flow. (iv) Cantilever and bluff body prism are in parallel.
Zhao et al. [56]; Yang et al. [32]	Piezoelectric	Square	2.5	—	8.4	8.0	Bluff body: 4 × 4 × 15 cm ³ ; cantilever: 15 × 3 × 0.06 cm ³	0.0346	(i) Experimentally determining for the first time that the square section is optimal for galloping energy harvesting compared to other shapes, giving the largest power and the lowest cut-in wind speed. (ii) High peak power is achieved, with high electromechanical coupling. (iii) Wide operational wind speed range.
Zhao et al. [57]	Piezoelectric	Square	1.0	—	4	5.0	Bluff body: 4 × 4 × 15 cm ³ ; cut-out cantilever: inner beam: 5.7 × 3 × 0.03 cm ³ ; outer beam: 17.2 × 6.6 × 0.06 cm ³ with cut out at the inner beam location	0.0162	(i) 2DOF cut-out structure with magnetic interaction. (ii) Reducing the cut-in speed. (iii) Enhancing output power in the low wind speed range. (iv) Having stiffness nonlinearity induced by magnetic interaction. (v) Output power is limited in high wind speeds.
Zhao and Yang [24]	Piezoelectric	Square	2.0	—	12	8.0	Bluff body: 4 × 4 × 15 cm ³ ; cantilever: 27 × 3.4 × 0.06 cm ³ ; beam stiffener: 8 × 4.5 × 0.5 cm ³	0.0455	(i) Employed beam stiffener as electromechanical coupling magnifier. (ii) Effective for all three types of harvesters based on galloping, vortex-induced vibration and flutter, with greatly enhanced output power. (iii) Displacement is not increased, thus not aggravating fatigue problem. (iv) Easy to implement. (v) Cut-in wind speed is undesirably increased.

TABLE 4: Continued.

Author	Transduction	Bluff body shape	Cut-in wind speed (m/s)	Cut-out wind speed (m/s)	Maximum power (mW)	Wind speed at max power (m/s)	Dimensions	Power density per volume (mW/cm ³)	Advantages/disadvantages and other information
Zhao et al. [33, 58]	Piezoelectric	Square	3.5	—	1.14	5.0	Bluff body: $2 \times 2 \times 10$ cm ³ ; cantilever: $13 \times 2 \times 0.06$ cm ³	0.0274	(i) Employed synchronous charge extraction (SCE) eliminates the requirement of impedance matching and ensures the flexibility of adjusting the harvester for practical applications. (ii) Saving 75% of piezoelectric materials by the SCE compared to the standard circuit. (iii) Achieving smaller transverse displacement and alleviating fatigue problem with SCE.
Zhao et al. [59, 60]	Piezoelectric	Square	3.0	—	3.25	7.0	Bluff body: $2 \times 2 \times 10$ cm ³ ; cantilever: $13 \times 2 \times 0.06$ cm ³	0.0782	(i) Synchronized switching harvesting on inductor (SSHI) enhances output power compared to standard circuit. (ii) SSHI shows more significant benefits in weak-coupling systems, yet loses benefits in strong-coupling conditions. (iii) Achieving 143% power increase at 7 m/s.
Bibo et al. [61]	Piezoelectric	Square	≈ 2.2	—	0.348 ^{*1}	4.5	Bluff body: $5.08 \times 5.08 \times 10.16$ cm ³ ; cantilever: $8.5 \times 0.7 \times 0.03$ cm ³	0.0013	(i) Concurrent flow and base excitations enhances energy harvesting. (ii) Base excitation improves electrical output in resonance region. (iii) Electrical output drops if base excitation frequency is close to but outside of resonance region.
Ewere and Wang [62]	Piezoelectric	Square	2	—	13	8	Bluff body: $5 \times 5 \times 10$ cm ³ ; cantilever: $22.8 \times 4 \times 0.04$ cm ³ ; bump stop: gap size: 0.5 cm, contact area: 1.27×4 cm ² ; location: 13 cm along cantilever	0.0512	(i) Incorporating an impact bump stop successfully relieves the fatigue problem. (ii) Achieving substantial 70% reduction in displacement amplitude with only 20% voltage reduction.

^{*1} Calculated by $(5.9 \text{ V})^2 / 100 \text{ k}\Omega$ from the information given in Table 1 and Figure 12 of the reference.

TABLE 5: Summary of various flutter energy harvester devices.

Author	Transduction	Flutter instability	Flap at the tip	Cut-in wind speed (flutter speed) (m/s)	Cut-out wind speed (m/s)	Maximum power (mW)	Wind speed at max power (m/s)	Dimensions	Power density per volume (mW/cm ³)	Advantages/disadvantages and other information
Bryant and Garcia [63]; Bryant and Garcia [26]	Piezoelectric	Modal convergence flutter	Airfoil, profile NACA0012	1.86	—	2.2	7.9	Airfoil: semichord 2.97 cm, span 13.6 cm. Cantilever: $25.4 \times 2.54 \times 0.0381$ cm ³	717×10^{-3}	(i) Semiempirical model of the nonlinear electromechanical and aerodynamic system accurately predicted electrical and mechanical response. (ii) Successfully predicts the flutter boundary with one of the real parts of the first two eigenvalues turning positive and the two imaginary parts coalescing. (iii) Wide operational wind speed range. (iv) Subcritical Hopf bifurcation, a large initial disturbance is fundamental for system startup.
				173	29	43	26	Flat plate tip: chord 3 cm, span 6 cm, thickness 0.79 mm. Cantilever: $7.6 \times 2.5 \times 0.0381$ cm ³	Stiff host structure 20.0 Compliant host structure 16.3	(i) Compared to a stiff host structure, a compliant host structure reduces the cut-in wind speed, cut-in frequency and oscillation frequency. (ii) The peak power is shifted toward the lower wind speeds with the compliant host structure.
				15.2	29	35	25	Flat plate tip: chord 3 cm, span 6 cm, thickness 0.79 mm. Cantilever: $7.6 \times 2.5 \times 0.0381$ cm ³	20.0	(i) Confirms the feasibility of using ambient flow energy harvesting to power aerodynamic control surfaces.
Bryant et al. [64]	Piezoelectric	Modal convergence flutter	Flat plate	173	29	43	26			
Bryant et al. [65]	Piezoelectric	Modal convergence flutter	Flat plate	173	29	43	26			
Erturk et al. [66]	Piezoelectric	Modal convergence flutter	Airfoil	9.30	—	10.7	9.30	Airfoil: semichord 12.5 cm, span 50 cm. Cantilever: —	2.27×10^{-3}	(i) Effect of electromechanical coupling on flutter energy harvesting is analyzed. (ii) Found that the optimal load gave the maximum flutter speed due to the associated maximum shunt damping effect during power extraction.
Sousa et al. [67]	Piezoelectric	Modal convergence flutter	Airfoil	12.1	—	12	12.1	Airfoil: semichord 12.5 cm, span 50 cm. Cantilever: —	Linear configuration 2.55×10^{-3} With free play nonlinearly 5.73×10^{-3}	(i) The free play nonlinearly reduces the cut-in wind speed and increased the output power. (ii) Theoretically determining that the hardening stiffness brings the response amplitude to acceptable levels and broadens the operational wind speed range.
Bibo and Daqaq [68]	Piezoelectric	Modal convergence flutter	Airfoil, profile NACA0012	2.3	—	0.138^{*1}	3 (With base acceleration 0.15 m/s^2)	Airfoil: semichord 4.2 cm, span 5.2 cm. Cantilever: —	8.38×10^{-4}	(i) Concurrent flow and base excitations enhances power generation performance. (ii) Concurrent excitations increases output power by 2.5 times below the flutter speed, and over 3 times above the flutter speed. (iii) Above the flutter speed, requiring careful adjustment because power is sensitive to base acceleration frequency.
Kwon [69]	Piezoelectric	Modal convergence flutter	Flat plate tip: Whole device T-shape	4	—	4.0	15	Flat plate tip: $6.0 \times 3.0 \text{ cm}^2$. Cantilever: $10.0 \times 6.0 \times 0.02$ cm ³	2.56	(i) Simple T-shape structure, easy to fabricate. (ii) No rotating components. (iii) Wide operational wind speed range.

TABLE 5: Continued.

Author	Transduction	Flutter instability	Flap at the tip	Cut-in wind speed (flutter speed) (m/s)	Cut-out wind speed (m/s)	Maximum power (mW)	Wind speed at max power (m/s)	Dimensions	Power density per volume (mW/cm ³)	Advantages/disadvantages and other information
Park et al. [70]	Electromagnetic	Modal convergence flutter	Flat plate tip; Whole device T-shape	4	—	1.1	8	Flat plate tip: $3.0 \times 2.0 \text{ cm}^2$ Cantilever: $4.2 \times 3.0 \times 0.01016 \text{ cm}^3$	5.82	(i) Determining that the onset of the harvester requires the load resistance to surpass the flutter onset resistance.
Li et al. [71]	Piezoelectric	cross-flow flutter	—	4	—	0.615	8	adhered double-layer, stalk: $72 \times 1.6 \times 0.041 \text{ cm}^3$	1.30	(i) Cross-flow configuration generated one order of magnitude more power than the parallel configuration. (ii) Having high power density per weight and per volume. (iii) Being robust, simple, and miniature sized. (iv) Being easy to blend in urban and natural environments due to its “leaf” appearance.
Deivasigamani et al. [72]	Piezoelectric	cross-flow flutter	Triangle	—	—	0.0883	8	Isosceles triangle tip: 8 cm in base, 8 cm in height, 0.35 mm in thickness. Stalk: $72 \times 1.6 \times 0.0205 \text{ cm}^3$	0.0651	(i) Determining that vertical stalk configuration is superior to the horizontal stalk with five times more output power.
Humdinger	Electromagnetic	cross-flow flutter	—	—	—	$\approx 9^{*2}$	10^{*3}	Membrane: $12 \times 0.7 \text{ cm}^2$ Casing: $13 \times 3 \times 2.5 \text{ cm}^3$	0.923	(i) Successfully powers wireless sensor nodes. (ii) Being compact and robust. (iii) Low cut-in wind speed and wide operational wind speed range.
Hobeck et al. [73]	Piezoelectric	Dual cantilever flutter	—	≈ 3	—	0.796	≈ 13	Two identical cantilevers: $14.6 \times 2.54 \times 0.0254 \text{ cm}^3$	0.422	(i) Very wide operational wind speed range with efficient power generation. (ii) Generating a significant amount of power from 3 m/s to 15 m/s when gap is small.

¹ Calculated by $18 \text{ mW/g} \times (0.15 \text{ m/s}^2 / 9.8 \text{ m/s}^2) / 2$ from the information given by the authors of the reference.^{2,3} Obtained from the figure in the datasheet of *μ*icroWindbelt (http://www.humdingerwind.com/pdf/microBelt_brief.pdf).

TABLE 6: Summary of various wake galloping energy harvester devices.

Author	Transduction	Prism shape	Cut-in wind speed (m/s)	Cut-out wind speed (m/s)	Maximum power (mW)	Wind speed at max power (m/s)	Dimensions	Power density per volume (mW/cm ³)	Advantages/disadvantages and other information
Jung and Lee [27]	Electromagnetic	Circular cylinder	≈1.2	—	370.4	4.5	Two identical cylinders: 5 cm in dia., 85 cm in length. Spacing distance: 5 × D = 25 cm.	0.111	(i) Determining the proper distance between the parallel cylinders for wake galloping energy harvesting, as 4-5 times the cylinder diameter, that is, $L/D = 4 \sim 5$. (ii) High output power. (iii) Wide operational wind speed range. (iv) Device volume is too big.
Abdelkefi et al. [74]	Piezoelectric	Windward: circular cylinder. Leeward: square cylinder	0.4	—	0.04~0.05	3.05	Circular cylinder: 1.25 cm in dia., 27.15 cm in length. Square cylinder: 1.28 × 1.28 × 26.67 cm ³ . Spacing distance: 24 cm. Piezoelectric two identical cantilevers: 15.24 × 1.8 × 0.0305 cm ³ .	5.72 × 10 ⁻⁴	(i) Power from a galloping square cylinder was greatly enhanced by wake effects of an upstream circular cylinder. (ii) Operational wind speed range was widened by wake galloping. (iii) Diameter of the upstream cylinder and the spacing distance between two cylinders require careful adjustment.

TABLE 7: Summary of various TIV energy harvester devices.

Author	Transduction	Cut-in wind speed (m/s)	Cut-out wind speed (m/s)	Maximum power (mW)	Wind speed at max power (m/s)	Dimensions	Power density per volume (mW/cm ³)	Advantages/disadvantages and other information
Akaydin et al. [47]	Piezoelectric	$\approx 5^{*1}$	—	0.55×10^{-4}	11	Bluff body: 3 cm in dia., 1.2 m in length. Cantilever: $3 \times 1.6 \times 0.02$ cm ³ . Distance from the wall: 4 cm	6.48×10^{-8}	(i) Performance of harvester in turbulent boundary layer depends on the distance from the wall; dominant oscillation frequency was close to the beam resonance frequency.
Hobeck and Inman [28]	Piezoelectric	$9 \sim 10^{*2}$	—	4.0	11.5	Bluff body: $4.45 \times 4.45 \times 10.92$ cm ³ . Four identical cantilevers in an array: 101.60 mm \times 25.40 mm \times 101.60 μ m steel substrate attached with 45.97 mm \times 20.57 mm \times 152.40 μ m PZT	0.0184	(i) The first TIV energy harvesting model with experimental validation. (ii) Being robust and survivable due to its inherent redundancy, with minor reduction in total power caused by one damaged element. (iii) Suitable for highly turbulent fluid flow environments like streams or ventilation systems.

*¹Obtained from the information of Figure 11 of the reference.*²Obtained from the information of Figure 7(b) of the reference.

TABLE 8: Summary of other types of energy harvester devices.

Author	Transduction	Cut-in wind speed (m/s)	Cut-out wind speed (m/s)	Maximum power (mW)	Wind speed at max power (m/s)	Dimensions	Power density per volume (mW/cm ³)	Advantages/disadvantages and other information
Bibo et al. [75]	Piezoelectric	$\approx 5.5^{*1}$	—	0.05	7.5	Cantilever: $5.8 \times 1.626 \times 0.038$ cm ³ . Chamber volume: 2300 cm ³	2.17×10^{-5}	(i) Mimicking the basic physics of music-playing harmonicas. (ii) Using optimal chamber volume and decreasing aperture's width reduce the cut-in wind speed.
Ovejas and Cuadras [76]	Piezoelectric	—	—	0.0002	12.3	Two identical bluff bodies: 0.5 cm in dia. Piezoelectric film: $15.6 \text{ cm} \times 1.9 \text{ cm} \times 40 \mu\text{m}$	1.25×10^{-5}	(i) Bluff body configuration outperformed the one fixed side and two fixed side configurations. (ii) Rotational turbulent flow from a dryer added to vortex shedding effects, giving higher electrical output than the laminar flow did.

*¹Obtained from the information of Figure 13(b) of the reference.

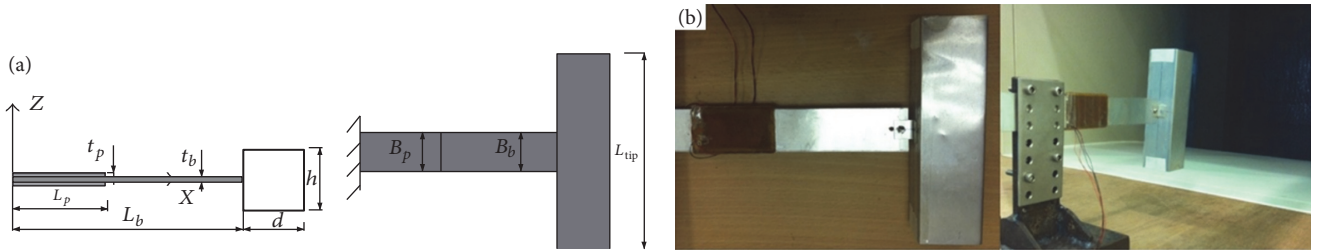


FIGURE 1: (a) Schematic and (b) fabricated prototype of galloping energy harvester with a square bluff body [32].

that the square section generates the largest power and has the lowest cut-in wind speed among all the considered sections. With a $150 \text{ mm} \times 30 \text{ mm} \times 0.6 \text{ mm}$ cantilever and a $40 \text{ mm} \times 40 \text{ mm}$ bluff body, a peak output power of 8.4 mW was measured at a wind speed of 8 m/s with the optimal load resistance, which is sufficient to power a commercial wireless sensor node. A 1DOF model was used which successfully predicted the power response. Moreover, the analysis with the galloping force represented with a seventh order polynomial predicted a hysteresis region of output power, which was not captured in the experiment due to the unavoidable turbulent flow component in the wind tunnel. It was recommended that the square section should be used for small-scale wind galloping energy harvesters.

Abdelkefi et al. [90] theoretically investigated the concept of using a galloping square cylinder to harvest energy. A normal form solution was provided to validate the numerical solution of the employed 1DOF model, with both solutions confirming that the instability of galloping is a supercritical Hopf bifurcation phenomenon. Theoretically, it was found that, for low Reynolds, the onset of galloping (cut-in wind

speed) and output power increased while the displacement decreased with the load resistance, while, for high Reynolds, there existed an optimal load with which maximum output power, maximum onset of galloping, and minimum displacement were achieved simultaneously. Abdelkefi et al. [91] considered more shapes of bluff body, including square, two isosceles triangles ($\delta = 30^\circ$ for one and $\delta = 53^\circ$ for the other, with δ being the base angle), and D-section. Theoretically, the isosceles triangle with $\delta = 30^\circ$ was recommended for small wind speeds while the D-section was recommended for high wind speeds. It should be noted that the aerodynamic coefficients used to calculate the galloping force are much sensitive to the flow condition (laminar or turbulent), which has great influences on the galloping behavior of different cross-sections. For example, turbulence in the flow can stabilize the square section, while it destabilizes the D-section. That is why the D-section cannot oscillate in the wind tunnel as shown by Zhao et al. [56], but it can gallop when placed in front of an axial fan [55].

In order to better understand the electroaeroelastic behaviors and provide a guideline to optimize the galloping

piezoelectric energy harvester, Zhao et al. [92] conducted a comparison of different modeling methods to weigh their validity, advantages, and disadvantages. The 1DOF model, single mode Euler-Bernoulli distributed parameter model, and multimode Euler-Bernoulli distributed parameter model were compared and validated with wind tunnel experiment on a prototype with a square sectioned bluff body. It was found that all these models can successfully predict the variation of the average power with the load resistance and the wind speed. Higher modes especially were found not necessary in modeling since minor difference was observed between the single mode and multimode Euler-Bernoulli distributed parameter models. It was concluded that the distributed parameter model has a more rational representation of the aerodynamic force while the 1DOF model gives a better prediction of the cut-in wind speed and owns its merit for conveniently obtaining the electromechanical coupling coefficient for a fabricated prototype via direct measurement. The parametric study showed that increasing the wind exposure area and decreasing the mass of the bluff body can increase the output power and reduce the cut-in wind speed. Moreover, in order to obtain the maximum power density (i.e., power per piezoelectric volume), it was suggested that a medium-long piezoelectric patch be used with careful sweep calculation.

A big issue of small-scale wind energy harvesting is that most piezoelectric aeroelastic energy harvesters operate effectively only at high wind speeds or within a narrow speed range. To overcome this issue, that is, to reduce the cut-in wind speed and enhance output power in the low wind speed range (e.g., lower than 5 m/s) which is typical for heating, ventilation, and air conditioning (HVAC) systems' flow condition, Zhao et al. [57] proposed a 2DOF piezoelectric galloping energy harvester with a cut-out cantilever and two magnets which induces stiffness nonlinearity of the whole system, as shown in Figure 2. Wind tunnel experiment confirmed its effectiveness, obtaining a reduced cut-in speed of 1 m/s and nearly four-time increase in power at 2.5 m/s with a magnet gap of 8 mm, as compared to the conventional 1DOF harvester. The total output power was found to be enhanced in the low wind speed range up to 4.5 m/s. It was concluded that the proposed 2DOF galloping harvester is suitable for powering wireless sensing nodes for indoor monitoring applications and highly urbanized areas with only low speed wind flows available. Subsequently, Zhao and her coworkers [24, 25, 33, 58–60] further enhanced the energy harvesting efficiency from both mechanical and circuit aspects by amplifying the electromechanical coupling with a beam stiffener and using nonlinear power extraction circuit, which will be reviewed with more details in Section 3.

Bibo and Daqaq [93, 94] established a universal relationship between the dimensionless output power and the dimensionless wind speed for galloping energy harvesters, which was shown to be only sensitive to the aerodynamic properties of the bluff body, but independent of the mechanical or electrical design parameters of the harvester. This relationship significantly facilitates the optimization analysis and comparison of performances of different bluff bodies. It was found that when all harvesters are optimally designed,

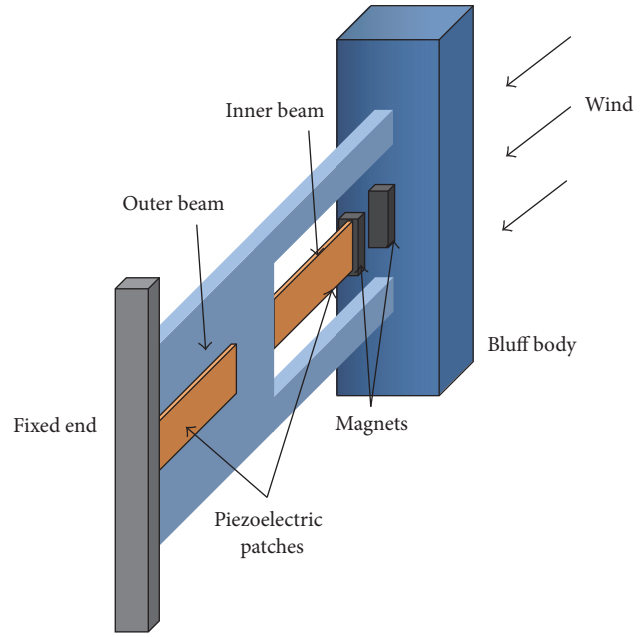


FIGURE 2: Schematic of 2DOF piezoelectric galloping energy harvester for power enhancement at low wind speeds.

a squared-section bluff body always outperformed the D-shaped and triangular sectioned bluff bodies, which agrees with the findings of Yang et al. [32] and Zhao et al. [56]. A 53° isosceles-triangular section harvester was found to outperform the D-shaped one at high wind speeds but underperform the D-shaped one at low wind speeds.

Daqaq [95] subsequently incorporated the actual wind statistics in the responses of galloping energy harvesters by fitting wind data using Weibull Probability Density Function (PDF). It was concluded that the wind speed statistics are essential for accurate load optimization. An exponentially correlated PDF was found to generate higher power than a Rayleigh distribution, which in turn produces higher power than a known wind speed located at the distribution average.

Ewere and Wang [62] employed the Krylov-Bogoliubov method to obtain analytical approximate solutions for galloping energy harvesters and found that the harvester with a square sectioned bluff body can outperform the rectangular sectioned one for all cases of load resistance and wind speed. In a subsequent study of Ewere et al. [96], a bump stop was introduced to relieve the fatigue problem of a galloping energy harvester. Using an optimal bump stop design with a gap size of 5 mm at the location of 130 mm along the beam of length 228 mm and a contact surface area of $12.7 \times 40 \text{ mm}^2$, a maximum 20% voltage reduction with substantial 70% reduction in limit cycle oscillation amplitude was observed from the wind tunnel experiment. It was concluded that the service life of a galloping harvester can be significantly improved by incorporating an impact bump stop.

Continuing the feasibility study of harvesting energy from transverse galloping conducted by Barrero-Gil et al. [88], Vicente-Ludlam et al. [97] carried out a theoretical study of a galloping electromagnetic energy harvester by

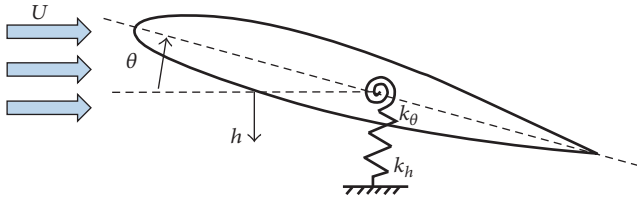


FIGURE 3: Schematic of an airfoil undergoing modal convergence flutter.

introducing the electromagnetic transduction mechanism into the 1DOF galloping system. It was found that, with the load resistance tuned to the optimal value for each wind speed, the power extraction efficiency can remain high over a larger range of wind speeds as compared to a fixed value of the load resistance. In a subsequent study, Vicente-Ludlam et al. [98] proposed a dual mass galloping electromagnetic energy harvesting system to enhance the energy extraction. It was shown theoretically that when the mechanical properties were properly adjusted, putting the electromagnetic generator between the secondary mass and a fixed wall or between the main and the secondary masses can improve the energy extraction efficiency and broaden the effective range of the wind speeds for energy harvesting. Table 4 presents a summary and quantitative comparison of the discussed harvesters based on galloping.

2.4. Energy Harvesters Based on Flutter. Numerous designs of energy harvesters based on flutter instabilities have been reported under axial flow conditions [99–105] or cross-flow conditions [71, 106], with flapping airfoil designs [63, 66, 107] or tree-inspired [71] and infrastructure-inspired designs [69]. Examples of flutter based harvesters include the wind belt [108] and flutter mill [109]. The main types of flutter based energy harvesters include those based on modal convergence flutter and those based on cross-flow flutter, which are reviewed in detail in the following sections. Moreover, a new type of flutter energy harvester named dual cantilever flutter [73] is also discussed.

2.4.1. Energy Harvesters Based on Modal Convergence Flutter.

Among the explosive studies on small-scale wind energy harvesting based on aeroelastic flutter, flapping airfoil or flapping wing based designs have been the most enthusiastically pursued. Schematic of an airfoil undergoing modal convergence flutter with coupled pitch-plunge motions is shown in Figure 3. Energy harvesting based on airfoil flutter has been reported a few decades ago by Bade [110] and McKinney and DeLaurier [111] using electromagnetic transduction mechanism. A patent has been filed by Schmidt [112] using two oscillating blades with piezoelectric transduction mechanism. The so-called “oscillating blade generator” was tested in a later study [113] and it was concluded that a power density of order 100 watts per cm^3 of piezoelectric material is theoretically possible to be achieved. In the recent years, along with the explosive research on energy harvesting with piezoelectric materials, piezoelectric wind

energy harvesting via airfoil flutter has become a hot research area with numerous studies reported.

Bryant and Garcia [26, 63] and coauthors [64, 65, 114–116] are among the very first to investigate the feasibility of piezoelectric energy harvesting with airfoil flutter. An airfoil flutter based energy harvester was first reported by Bryant and Garcia [63] with both wind tunnel experimental results and theoretical predictions and further studied with a more detailed theoretical modeling process [26]. A piezoelectric bimorph was connected to a rigid airfoil (NACA0012 airfoil profile) at the tip with a revolute joint, permitting both transverse and rotary displacement of the airfoil. Theoretical analyses were carried out to predict behaviors of the harvester at the flutter boundary with linear models and during limit cycle oscillations above the flutter boundary with nonlinear models. The linear mechanical model incorporating electromechanical coupling was established using the energy method based on the Hamilton’s principle, while the linear aerodynamic model was established based on the finite-state unsteady thin-airfoil theory of Peters et al. [117]. Small angle and attached flow assumptions were taken in the linear models. For the nonlinear models, large flap deflection angles and flow separation effects were taken into account. Wind tunnel experimental results of a fabricated harvester prototype agreed well with the analytical predictions. The prototype consisted of a $254 \times 25.4 \times 0.381$ mm substrate cantilever attached with two PZT patches of dimension $46.0 \times 20.6 \times 0.254$ mm, and an airfoil with a semichord of 2.97 cm and a span of 13.5 cm. A cut-in wind speed of 1.86 m/s was obtained. A maximum output power of 2.2 mW was delivered to an optimal load of 277 k Ω at a wind speed of 7.9 m/s. It was concluded that collating and superposing the bender and system resonances can maximize the output power.

In a subsequent work of Bryant et al. [114], a parameter study was performed both experimentally and analytically to investigate the influence of several system design parameters on the cut-in wind speed. It was found that the cut-in wind speed could be minimized by modifying the hinge stiffness and the flap mass distribution, yet its variation was less sensitive to the hinge stiffness when large damping was introduced. Later, Bryant et al. [115] compared the quasi-steady aerodynamic model with the semiempirical model considering dynamic stall effects. It was concluded that the quasi-steady model was applicable only for low flapping frequencies, while the dynamic stall model can be used to predict trustworthy results at high frequencies. Bryant et al. [64] also investigated the influence of the compliance of the host structure on the behavior of the airfoil flutter based energy harvester. Experimentally, it was found that a compliant host structure reduced the cut-in wind speed, cut-in frequency, and oscillation frequency during the limit cycle oscillation and shifted the peak power toward the lower wind speeds, as compared to a stiff host structure. Bryant et al. [116] presented an experimental study on energy harvesting efficiency and found that the peak power density and power extraction efficiency of the flutter energy harvester occurred at the lowest wind tested, due to the small swept area of the device. At that wind speed which was near the flutter boundary, the limit cycle oscillation frequency matched the

first natural frequency of the piezoelectric structure. When the wind speed increased, the output power, the swept area of the device, and available power in the flow also increased, but power density and power extraction efficiency decreased. Preliminary study of implementing synchronized switching approaches like the synchronized switching and discharging to a storage capacitor through an inductor (SSDCI) technique in an aeroelastic flutter energy harvester was conducted, with a separate microcontroller working as the peak detector. However, the efficiency increasing capability of the SSDCI in flutter energy harvesting was not thoroughly studied. Subsequently, Bryant et al. [65] experimentally demonstrated the concept of using ambient flow energy harvesting to power aerodynamic control surfaces. With a prototype that produced a power of 43 mW at a wind speed of 26 m/s, it was shown that the system produced more than 55° of tab deflection over approximately 0.7 seconds after the storage capacitor was charged for 235 seconds at 32.2 m/s. It was found that the harvester was still able to produce power when the host control surface was rotated to a large angle of attack over 50°, confirming the feasibility of the alternative design of placing the harvester on the control surface itself.

Erturk and coauthors [66, 67, 118–121] are also among the first to study harnessing flow energy via the aeroelastic flutter of airfoils. The concept of energy harvesting from macrofiber composites with curved airfoil section was first proposed by Erturk et al. [118]. Later, Erturk et al. [66] presented an experimentally validated lumped-parameter aeroelastic model for the flutter boundary condition. The linear lift and moment at flutter boundary were modeled with the Theodorsen's unsteady thin airfoil theory. Using a flexibly supported airfoil prototype with a semichord of 0.125 m and a span length of 0.5 m, a power of 10.7 mW was measured at the linear flutter speed of 9.30 m/s with an optimal load of 100 k Ω . It was found both theoretically and experimentally that the optimal load gave the maximum flutter speed due to the associated maximum shunt damping effect during power extraction. It was recommended that a nonlinear stiffness component and/or a free play can be incorporated to induce stable limit cycle oscillations above and below (in the case of subcritical Hopf bifurcation) the flutter boundary for useful power generation. In order to obtain stable limit cycle oscillations above or below the flutter boundary, nonlinearity has to be introduced into the system, which can be either structural nonlinearity or aerodynamic nonlinearity. The structural nonlinearity suggested by Erturk et al. [66] and the aerodynamic nonlinearity modeled in Bryant and Garcia [26] can both ensure the acquisition of stable and large-amplitude limit cycle oscillations beyond the linear flutter speed and harvest energy in a wide wind speed range.

In a subsequent study, Sousa et al. [67] theoretically and experimentally investigated the advantages of exploiting structural nonlinearities in the piezoaeroelastic energy harvesting system. Piezoelectric coupling was introduced to the plunge DOF while structural nonlinearities were introduced to the pitch DOF, aiming to solve the problem of a linear piezoaeroelastic energy harvester, that is, having persistent oscillations only at the flutter boundary thus leading to a

very limited condition for energy harvesting. It was shown both theoretically and experimentally that the free play nonlinearity reduced the cut-in wind speed by 2 m/s and doubled the output power. Theoretically, it was found that the hardening stiffness helped to broaden the operational wind speed range. It was concluded that the combined structural nonlinearities can be introduced to enhance the performance of aeroelastic energy harvesters based on piezoelectric and other transduction mechanisms.

De Marqui and Erturk [119] theoretically analyzed the performance of two airfoil-based aeroelastic energy harvesters with piezoelectric and electromagnetic couplings inserted to the plunge DOF separately. It was found that optimal values of load resistance giving the largest flutter speed as well as the maximum output power for the considered range of dimensionless equivalent capacitance and dimensionless electromechanical coupling in the piezoelectric configuration existed. For the electromagnetic configuration, increasing the load resistance reduced the flutter speed for any dimensionless inductance or electromechanical coupling, and the optimum load resistance matched the internal coil resistance, which agreed with the maximum power transfer theorem.

Subsequently, Dias et al. [120] theoretically analyzed the performance of a hybrid airfoil-based aeroelastic energy harvester using simultaneous piezoelectric and electromagnetic induction. It was shown that, in the electromagnetic induction, the internal coil resistance affected the flutter speed and deteriorated the performance of the system. The parameter study showed that the combination of low dimensionless radius of gyration, low pitch-to-plunge frequency ratio, and large dimensionless chord-wise offset of the elastic axis from the centroid enhanced the performance by increasing the output power as well as decreasing the cut-in wind speed.

Later, Dias et al. [121] continued the study of the hybrid aeroelastic energy harvester with combined piezoelectric and inductive couplings based on a 3DOF airfoil. A control surface was introduced, bringing in a third displacement, that is, the control surface displacement. Theoretical parametric study showed that increasing the dimensionless radius of gyration, dimensionless chord-wise offset of the elastic axis from the centroid, and control surface pitch-to-plunge frequency ratio and decreasing the pitch-to-plunge frequency ratio increased the power output and reduced the cut-in speed. It was concluded that the 3DOF configuration enhanced the performance of the harvester by offering a broader design space and set of parameters for system optimization.

Earliest studies of airfoil-based aeroelastic energy harvesters also include the work of Abdelkefi et al. [107, 122]. Abdelkefi et al. [122] theoretically investigated the performance of an airfoil-based piezoaeroelastic energy harvester with the method of normal form, which was validated by the numerical integrations. It was found that the system's instability to the subcritical type depended significantly on the cubic nonlinearity of the torsional spring. In a subsequent study, Abdelkefi et al. [107] implemented two linear velocity feedback controllers to reduce the flutter speed to any desired value and hence generate energy from limit cycle oscillations at any desired low wind speed. This was realized

by introducing two vibration velocity dependent terms into the system governing equations. It was found theoretically that the aerodynamic nonlinearity produced a supercritical bifurcation while the cubic stiffness nonlinearity produced supercritical or subcritical bifurcation depending on whether the stiffness nonlinearity was hard or soft.

Instead of harvesting energy only from flowing wind, Bibo and Daqaq [123] theoretically investigated the performance of an airfoil-based piezoaeroelastic energy harvester which concurrently harvested energy from ambient vibrations and wind, by introducing harmonic base excitation in the plunge direction. The nonlinear aerodynamic lift and moment were modeled with the quasi-steady approximation. Cubic nonlinearities were introduced for the plunge and pitch. Complex motions were predicted under the combined excitations by analytical solutions based on the normal form method, which were validated by numerical integrations. In a subsequent study, Bibo and Daqaq [68] performed experiment to demonstrate these complex motions by attaching the harvester prototype to a seismic shaker which provided the harmonic base excitation and putting the whole system in a wind tunnel which provided the aerodynamic loads. Below the flutter speed, it was found that the flow serves to amplify the output power from base excitations. Beyond the flutter speed, the power was enhanced when the excitation frequency was right above resonance, while it dropped when the excitation frequency was slightly below resonance. It was concluded that the harvester under combined excitations was superior to that under one type of excitation. The output power was improved by over three times compared to that from an aeroelastic harvester and a vibration harvester together.

Bae and Inman [124] analyzed the performance of an airfoil-based piezoaeroelastic energy harvester with the root-locus method and time-integration method. It was found that energy can be harvested from stable LCOs when the frequency ratio was larger than 1.0 in a wide range of wind speeds below the flutter speed for free play nonlinearity and over the flutter speed for cubic hardening nonlinearity.

Wu and his coworkers [125] (Xiang et al., 2015) theoretically investigated the performance of an airfoil-based piezoaeroelastic energy harvester with free play nonlinearity and showed that the amplitudes of pitch and plunge motions as well as output power increased with the free play gap, with the power and the gap having an approximate linear relationship in particular. Moreover, it was found that discrete gusts in the incoming flows influenced the phase of the dynamic and electrical responses, yet they had no influence on the electrical output amplitude. For other studies of wind energy harvesting from flapping foils, readers are referred to the excellent review work of Young et al. [30] and Xiao and Zhu [20], in which the authors inspected flapping foil power extraction from a mathematical aeroelastic perspective with a different literature coverage from that of this paper. They are recommended to readers as complementary materials with the reviews in this section.

Different from the utilization of airfoils attached to cantilever tips, Kwon [69] experimentally investigated the performance of a T-shaped piezoelectric cantilevered energy

harvester. The T-shape resembled a half H-sectional shape of the Tacoma Narrow Bridge which collapsed in 1940 due to large amplitude aeroelastic flutter. The T-shape cantilever underwent coupled bending and torsional motions in wind flows. Using a prototype with $L \times B \times H = 100 \times 60 \times 30$ mm, a 0.2 mm thick aluminum substrate, and six attached PZT patches of 28×14 mm for each, a flutter speed of 4 m/s and a maximum power of 4.0 mW at a wind speed of 15 m/s were measured with a load of 4 M Ω . Annual output energy of 4.3 Wh was calculated at an assumed mean wind speed of 5 m/s. It was concluded that it had the potential to power a mobile electronic apparatus cost-effectively with a series of the proposed harvesters.

Subsequently, Park et al. [70] continued the study of T-shaped cantilever where electromagnetic transduction was employed. It was found experimentally that the onset of the harvester occurred only when the load resistance surpassed a certain value, that is, the flutter onset resistance. CFD simulations were performed to estimate the aerodynamic damping and thus predict the flutter onset resistance, which agreed well with experiment. Using a prototype of $42 \times 30 \times 20$ mm with a 0.1016 mm thick cantilever substrate, a maximum power of around 1.1 mW was delivered to a 1 k Ω load at a wind speed of 8 m/s.

Modal convergence flutter based energy harvester designs also include the work of Boragno et al. [126]. In their design, a wing was attached to a support by two elastomers with one for each side, which provided bending and torsional stiffness at the same time. Influences of parameters including the elastomer elastic constant, wing mass, position of mass center, and elastic attachment point on oscillation responses were investigated. The self-sustained oscillations with properly adjusted parameters were concluded to be suitable for energy harvesting purpose though no specific transduction mechanism was proposed. A similar device called flutter mill has been demonstrated by Sharp [109] with electromagnetic transduction.

2.4.2. Energy Harvesters Based on Cross-Flow Flutter. Inspired by the natural flapping leaves in the tree subject to ambient flows, Li and Lipson [127] proposed a device consisting of a PVDF stalk, a plastic hinge, and a triangular polymer/plastic "leaf." Two configurations were investigated with different direction arrangements of the stalk, that is, the horizontal-stalk leaf and the vertical-stalk leaf. The horizontal-stalk underwent bending motion while the leaf underwent coupled bending and torsional motions around the hinge, that is, modal convergence flutter, similar to the airfoil-based piezoaeroelastic energy harvester. The vertical-stalk, where the long axes of the stalk were perpendicular to the incoming flow, underwent cross-flow flutter, which was demonstrated more clearly in a subsequent study of Li et al. [71] with more experiments performed. It was found that, compared to the parallel configuration, the cross-flow configuration increased the power by one order of magnitude. Performances of different leaf's shapes, different leaf's area, different stalk scales (short, long, and narrow-short), and different PVDF layer configurations (single-layer, adhered double-layer, and air-spaced double-layer) were measured and compared. It

was found that the circle, square, and equilateral triangle shapes of leaf had similar and the best performance, and the cut-in wind speed and peak power increased with leaf's area. Stalk scale and PVDF layer configuration affected the power with a nonmonotonous, complex behavior. A peak power of $615 \mu\text{W}$ was obtained with an adhered double-layer stalk of $72 \times 16 \times 0.41 \text{ mm}$ at 8 m/s on a $5 \text{ M}\Omega$ load and the maximum power density of $2036 \mu\text{W}/\text{m}^3$ was obtained with a unimorph narrow-short stalk of $41 \times 8 \times 0.205 \text{ mm}$ at 7 m/s on a $30 \text{ M}\Omega$ load. It was concluded that although the proposed device had low-power density compared to commercial wind turbines, it owned advantages of being robust, simple, miniature sized, and able to blend in urban and natural environments.

Analyses of flapping-leaf energy harvesters were also performed by McCarthy et al. [128, 129] with smoke-flow visualization and tandem harvester arrangements and coauthors Deivasigamani et al. [72] with a parallel-flow asymmetric configuration, where the offset of the leaf axes from the stalk axes induced torsional motions of stalk around axis x . It is actually a modal convergence flutter based harvester, yet due to the similar constructions to those by Li and Lipson [127], we put its reviews in this section of cross-flow flutter. The PVDF partly operated in the d_{32} mode which had a low piezoelectric conversion coefficient; therefore, it was concluded that power from torsion (d_{32}) in parallel flow configuration acted only as a low-value peripheral supplement to that from bending. The output was similar to that of a parallel flow flapping-leaf harvester, much lower than that of a cross-flow counterpart harvester.

Studies on energy harvesting from cross-flow flutter were also conducted by De Marqui Jr. et al. [106, 130], aiming at harvesting energy with the wings of unmanned air vehicles (UAVs). Using an electromechanically coupled finite element (FE) model, a preliminary study was performed by De Marqui Jr. et al. [131] on a plate with embedded piezoceramics under base excitations with no air flows. Subsequently, aerodynamic loads were introduced to the plate to simulate the condition during flight by De Marqui Jr. et al. [130] using coupled FE model and unsteady vortex-lattice model to predict the electric outputs. In a later study of De Marqui Jr. et al. [106], segmented electrodes were used to avoid cancellation of electrical output during typical coupled bending-torsion aeroelastic modes. It was found that the peak power from the segmented electrode was larger than that from the continuous electrode for all considered load resistance at a flutter speed of 40 m/s . Torsional motions of the coupled modes were found to become relatively significant for segmented electrodes, associated with improved broadband performance and increased flutter speed.

Cross-flow flutter based energy harvesters also include the patented windbelt that was produced by Humdinger Wind Energy, LLC [108], which extracts wind energy using electromagnetic transduction with a properly tensioned flexible belt undergoing flutter motions when subjected to flows.

2.4.3. Energy Harvesters Based on Dual Cantilever Flutter. Finally, a novel type of flutter termed "dual cantilever flutter" different from the above-mentioned cases was reported and analyzed for energy harvesting purpose by Hobeck et al. [73].

Two identical cantilevers were found to undergo large amplitude and persistent vibrations when subject to wind flows, which can be utilized for energy harvesting purpose. Two identical cantilevers of $14.6 \times 2.54 \times 0.0254 \text{ cm}^3$ were employed in the wind tunnel experiment setup. The gap distance was found to affect the power output significantly. For small gap distances between 0.25 cm and 1.0 cm , the cantilevers produced a significant amount of power over a very large range of wind speeds from 3 m/s to 15 m/s . A maximum power of 0.796 mw was achieved at 13 m/s . It was concluded that dual cantilever flutter phenomenon is an attractive and robust energy harvesting method for highly unsteady flows. A comparison of the reported flutter harvesters is presented in Table 5 with regard to their quantitative performance as well as the merits, demerits, and applicability.

2.5. Energy Harvesters Based on Wake Galloping. Wind energy extraction exploiting wake galloping phenomenon was studied by Jung and Lee [27]. They developed a device consisting of two paralleled cylinders to extract power from the leeward cylinder, which oscillated due to the wakes from the windward cylinder. Electromagnetic transduction was employed. It was found that with proper distance (4-5 times the cylinder diameter) between the parallel cylinders, the leeward cylinder could oscillate with considerable magnitude. With two cylinders of 5 cm in diameter and 0.85 m in length with a space of 25 cm in between, an average output power of $50\text{--}370 \text{ mW}$ was measured under a wind speed of $2.5\text{--}4.5 \text{ m/s}$ with different coil and spring configurations. Piezoelectric energy harvesting could also utilize the wake galloping with proper arrangement of parallel cylinders based on these results.

Abdelkefi et al. [74] enhanced the performance of a galloping energy harvester with the wake galloping phenomenon by placing a circular cylinder in the windward direction of a square galloping cylinder. It was found experimentally that the range of wind speeds for effective energy harvesting can be widened by the wake effects of the upstream cylinder. With an upstream cylinder 27.15 cm in length and 1.25 cm in diameter, the power from the square cylinder was greatly enhanced when the spacing was larger than 16 cm , especially from 2.58 m/s to 3.51 m/s where the single square cylinder generated no power without the introduced wake galloping effects. With a spacing distance of 24 cm , a peak power of $40\text{--}50 \mu\text{W}$ was measure at 3.05 m/s . It was concluded that enhanced galloping energy harvesters can be designed by utilizing wake galloping effects, with properly designed dimension, spacing distance, and load resistance. Table 6 summarizes the reported harvesters based on wake galloping.

2.6. Energy Harvesters Based on Turbulence-Induced Vibration. A big problem of the above-mentioned harvesters is that most of them oscillate and generate energy only in laminar flow conditions, which are usually not the case in natural environment where turbulence exists thus stabilizing the harvesters. Also, they require a cut-in speed as the minimum limit of wind speed, below which no power can be generated. Yet turbulence-induced vibrations (TIVs) never

vanish even with very small average wind speed, which could be utilized by energy harvesters based on TIVs [28, 132].

Akaydin et al. [47] experimentally investigated the performance of a cantilevered harvester placed in turbulent boundary layer flow near the bottom wall of a wind tunnel. It was found that electrical output monotonically increased with the wind speed. With a boundary layer thickness of $\delta = 115$ mm, the global and local maxima of power were observed independent of wind speed at $h = 40$ mm and 75 mm, respectively, which were far away from the maximum turbulent kinetic energy location of around 8 mm. Time domain signals of voltage showed that the dominant frequency of 46 Hz was close to the resonance frequency of the beam, while the secondary dominant frequency was around 317 Hz near the turbulence frequency of 275 Hz, leading to the conclusion that higher frequency excitations due to turbulence existed in TIVs.

Hobeck and Inman [28] proposed the concept of harvesting energy from highly turbulent flows with “piezoelectric grass” consisting of an array of generating elements in the highly turbulent wake of a bluff body or in entirely turbulent fluid flows. A combination technique of electromechanical modeling for the structure and statistical modeling for the turbulent induced forces was proposed, which was the first documented experimentally validated TIV energy harvesting model. Experimentally, a peak power output of 1.0 mW per cantilever was measured for the four-element harvester array fabricated with PZT ($101.60 \text{ mm} \times 25.40 \text{ mm} \times 101.60 \mu\text{m}$ steel substrate attached with $45.97 \text{ mm} \times 20.57 \text{ mm} \times 152.40 \mu\text{m}$ PZT) at a mean wind speed of 11.5 m/s and a load of 49.2 k Ω . A peak power of 1.2 μW per cantilever was measured at 7 m/s on a 4.70 M Ω load for the six-element array with PVDF ($72.60 \text{ mm} \times 16.20 \text{ mm} \times 178.00 \mu\text{m}$ Mylar substrate attached with $62.00 \text{ mm} \times 12.00 \text{ mm} \times 30.00 \mu\text{m}$ Piezo film). The main advantage was concluded to be in its robustness and survivability due to its inherent redundancy since only minor reduction in total power happened if one element was damaged. Table 7 presents a comparison of the discussed harvesters based on turbulence-induced vibration.

2.7. Other Small-Scale Wind Energy Harvester Designs. With designs different from the above-mentioned cases, recent progress on energy harvesting from wind flows also includes a damped cantilever pipe carrying flowing fluid [133], a harmonica-type aeroelastic micropower generator [75], a tensioned piezoelectric film facing laminar and/or turbulent incoming flows [76], a hinged-hinged piezoelectric beam facing turbulent airflows [134], and a micromachined piezoelectric airflow energy harvester inside a Helmholtz resonator [135].

Bibo et al. [75] proposed a harmonica-type micropower generator consisting of a cantilever embedded within a cavity. Pressure from the incoming flow caused deflection of the cantilever, generating a small gap which in turn reduced the flow pressure. The periodic fluctuations in the pressure induced the beam to undergo self-sustained oscillations. It was found that using optimal chamber volume and decreased aperture's width reduced the cut-in wind speed. The optimal load for maximum power did not vary considerably with

the inflow rate. With a $58 \times 16.26 \times 0.38$ mm piezoelectric cantilever, an average power of 55 μW was obtained at an average wind speed of 7.5 m/s.

Ovejas and Cuadras [76] investigated the energy harvesting performances of a PVDF film generator with three different setup configurations. In the bluff body configuration of setup (a), two cylindrical bluff bodies of 0.5 cm diameter are attached to the PVDF film in the windward direction, with the wind flowing parallel with the surface film, while in the other two configurations with one or two ends fixed, that is, setup (b) and (c), the wind flows perpendicularly to the surface film. Experiment showed that the turbulent flow from a hairdryer gave a higher voltage than the laminar flow from a wind tunnel did. It was explained that the rotational turbulent flow was added to the vortex shedding from the two bluff bodies, thus enhancing power generation. With performance comparison, setup (a) outperformed the other two and was recommended for energy harvesting. A maximum power of 0.2 μW was measured with a setup (a) film that was 15.6 cm in length, 1.9 cm in width, 40 μm in thickness, and 9.9 nF in capacitance. The power is relatively low compared to other studies. To improve the performance, future studies were recommended to optimize the oscillation and resonant frequency coupling. Table 8 presents a comparison of the discussed other types of small-scale wind energy harvesters.

3. Enhancement Techniques Involved in Small-Scale Wind Energy Harvesting Systems

3.1. Enhancement with Modified Structural Configurations. In the literature, various methods have been proposed to improve the efficiency of power output for the vibration-based piezoelectric energy harvesters. The beam configuration can greatly influence the strain distribution throughout the harvester, resulting in significant difference in power generation. For example, a trapezoidal cantilever harvester can generate more than twice power than the rectangular one [136]. The multimodal techniques can enlarge the bandwidth of operating frequencies of the vibration-based energy harvesters, for example, the piezoelectric energy harvester with a dynamic magnifier [137] and the 2DOF energy harvester with closed first and second mode frequencies [138, 139]. With frequency upconversion techniques, the low-frequency ambient vibration can be transferred to high frequency vibrations, providing a frequency-robust energy harvesting solution for the low frequency oscillations [140].

In the area of wind energy harvesting, some techniques have also been proposed to enhance the power extraction performance from the mechanical aspects with modified structural designs. For example, utilizing the frequency upconversion mechanism, Zhao et al. [57] used a 2DOF cut-out structure with magnetic interaction to enhance the output power of a galloping harvester in the low wind speed range.

Recently, researchers have been employing the base vibratory excitation as a supplementary energy source to enhance energy harvesting from aerodynamic forces. The efforts have been devoted to energy harvesting from airfoil aeroelastic

flutter [68, 123], VIV [141, 142], and galloping [143]. The work of Bibo and Daqaq [68, 123] has been reviewed in Section 2.4.1. Dai et al. [142] numerically investigated the responses of a cantilevered VIV harvester under combined VIV and base vibrations. Using a single piezoelectric energy harvester under combined excitations was reported to improve the power compared to using two separate harvesters when the wind speed was in the synchronization region. Responses of a fluid-conveying riser under concurrent excitations were also studied [141]. Numerically, it was found that the response changed from aperiodic to periodic motions when the wind speed approached the synchronization region. It was stated that increased base acceleration induces a wider synchronization region. Energy harvesting from concurrent galloping and base excitations was numerically investigated by Yan et al. [143]. Widened synchronization region was also found to occur with increased base acceleration.

Stiffness nonlinearity (monostable, bistable, or tristable) has been frequently introduced to vibration-based energy harvesters in order to broaden the operating bandwidth thus to adapt to environments with broadband or frequency-variant vibrations [144–147] (Tang and Yang, 2012). In wind energy harvesting, stiffness nonlinearity has also been employed, instead of broadening bandwidth, to reduce the cut-in wind speed and enhance power output. Free play or cubic stiffness nonlinearities have been employed by Sousa et al. [67], Bae and Inman [124], and Wu et al. [125] to enhance energy harvesting from airfoil flutter. Moreover, the influence of monostable and bistable nonlinearity on galloping energy harvesting has been investigated by Bibo et al. [148]. It was shown that the bistable harvester outperforms the monostable harvester when interwell oscillations are excited.

Zhao and Yang [24] reported an easy but quite effective way to increase the power extraction efficiency of aeroelastic energy harvesters, by adding a beam stiffener to amplify the electromechanical coupling as shown in Figure 4. It was theoretically explained that the beam stiffener increases the slope of the beam's fundamental mode shape and thus works as an electromechanical coupling magnifier and enhances the output power. Theoretical analysis showed that this method is effective for all three types of harvesters based on galloping, vortex-induced vibration, and flutter. Compared to the conventional designs without the beam stiffener, the enhanced designs gave dozens of times increase in power, almost 100% increase in the power extraction efficiency, and comparable or even smaller transverse displacement. Experimentally, a maximum output power of around 12 mW was measured at 8 m/s from a galloping harvester prototype with the beam stiffener, much larger than that of around 2 mW from the conventional counterpart. The shortcoming is that the cut-in wind speed was undesirably increased with the beam stiffener.

Other efforts on structural modifications include attaching the cylindrical bluff body to the beam instead of separating them to enhance the effects of vortex shedding [23] and adding a movable mass to adjust the resonance frequency thus broadening the functional wind speed range of a harvester based on vortex-induced vibrations [49], which have been mentioned in Section 2.2.

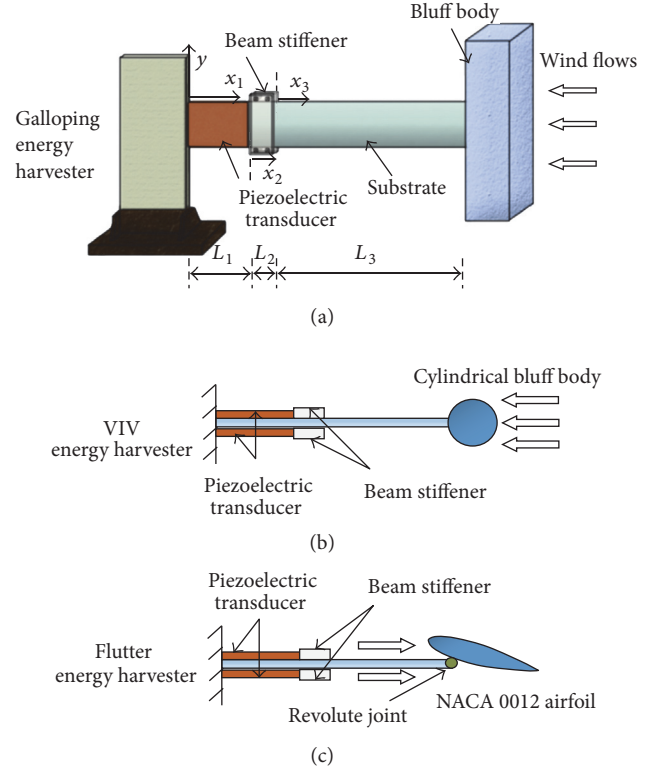


FIGURE 4: Configurations of enhanced energy harvesters with the beam stiffener, based on, from (a) to (c), galloping, VIV, and airfoil flutter [24].

3.2. Enhancement with Sophisticated Interface Circuits. In the field of VPEH, many power conditioning circuit techniques have been developed to regulate and enhance power transfer from the piezoelectric materials to the terminal load or storage components, including the impedance adaptation [149, 150], synchronized switch harvesting on inductor (SSHI) [151–157], synchronous charge extraction (SCE) [155, 158–160], and energy storage circuits [161, 162]. However, very limited researches have been reported on the integration of advanced interfaces with aeroelastic energy harvesters to enhance their power output.

Enhancing power generation performance of wind energy harvesters with modified interface circuits has been considered by Taylor et al. [43]. They implemented a switched resonant-power converter, which was similar to a series SSHI yet without the full wave rectifier in an oscillating piezoelectric eel. Robbins et al. [44] implemented a quasi-resonant rectifier in a flapping PVDF (similar to eel), and Bryant et al. [116] employed an SSDCI circuit with a separate microcontroller based peak detection system in an airfoil-based piezoelectric flutter energy harvester. De Marqui Jr. et al. [106] used a resistive-inductive circuit to extract energy from a fluttering bimorph plate under cross-flow condition and showed that the power output was enhanced to about 20 times larger than the case with a pure resistor in the circuit at the short circuit flutter speed and short circuit flutter frequency.

Zhao et al. [33, 58] investigated the feasibility of employing a self-powered SCE interface to enhance the performance

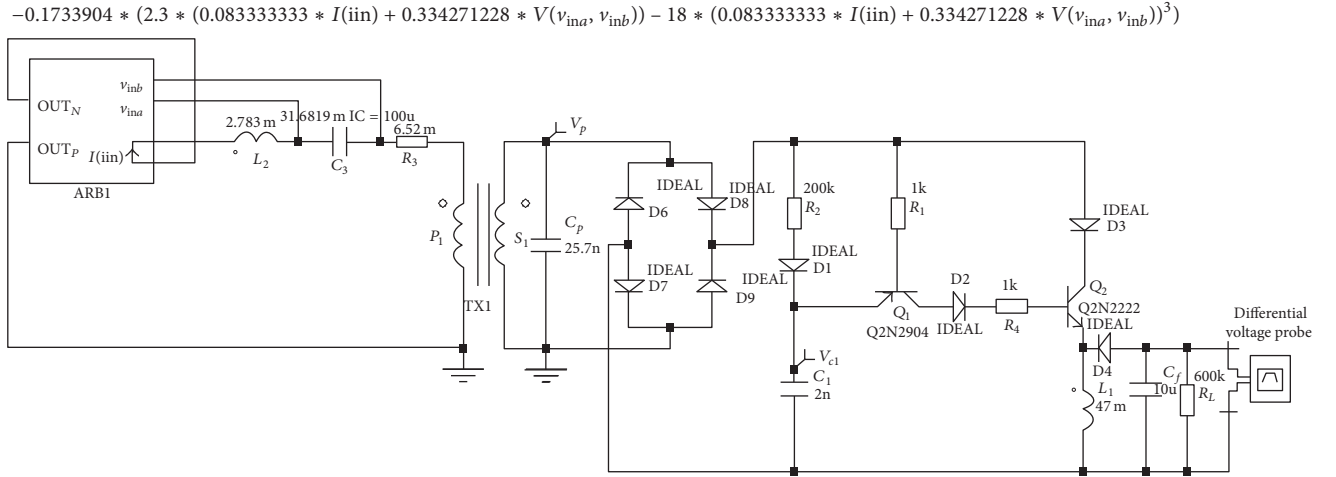


FIGURE 5: Schematic of self-powered SCE circuit integrated with a galloping piezoelectric energy harvester [33].

of a galloping-based piezoelectric energy harvester, as shown in Figure 5 depicting the equivalent circuit model (ECM) of harvester and the SCE diagram. Experimental and theoretical comparison of the performance of SCE with a standard circuit revealed three main advantages of SCE in galloping-based harvesters. Firstly, SCE eliminates the requirement of impedance matching and ensures the flexibility of adjusting the harvester for practical applications, since the output power from SCE is independent of electrical load. Secondly, 75% of piezoelectric materials can be saved by the SCE compared to the standard circuit. Thirdly, the SCE helps to alleviate the fatigue problem with a smaller transverse displacement during harvester operation.

Zhao and Yang [25] further proposed the analytical solutions of responses of a galloping-based piezoelectric energy harvester. Explicit expressions of power, voltage, displacement amplitude, optimal load, and electromechanical coupling as well as cut-in wind speed for the simple AC, standard, and SCE circuits were derived, which were validated with wind tunnel experiments and circuit simulation. It was found that the three circuits generated the same maximum power but the SCE achieved it with the smallest coupling value. Moreover, the SCE was found to give the smallest displacement and highest cut-in wind speed, while the standard circuit was found to have the largest displacement and lowest cut-in speed. It was concluded that the SCE is suitable for the cases with small coupling and relative high wind speeds, while the AC and standard circuit are suitable for large coupling cases. With the AC and standard circuits, small loads are better for cases requiring high current, such as charging batteries, and large loads suit the conditions having high threshold voltages. Subsequently, Zhao et al. [59, 60] investigated the capability of enhancing power output of a galloping-based piezoelectric energy harvester with the SSHI interfaces. Experimentally, it was found that the SSHI circuit achieves tremendous power enhancement in a weak-coupling system, and the enhancement is more significant at higher wind speeds. A power increase of 143% was obtained with

the SSHI at 7 m/s for a weak-coupling harvester. However, the SSHI circuits lost the advantage strong-coupling conditions.

4. Application of Small-Scale Wind Energy Harvesting in Self-Powered Wireless Sensors

Many studies in vibration energy harvesting have investigated the feasibility of extracting energy from ambient vibrations to implement self-powered wireless sensors. Similarly, a main purpose of small-scale wind energy harvesting is to power the wireless sensors placed in an airflow-existing environment with the extracted flow power.

Flammini et al. [163] demonstrated the viability of harvesting small-scale wind energy to power autonomous sensors in air ducts used for heating, ventilating and air-conditioning (HVAC). To demonstrate the concept, a small-scale wind turbine with a commercial electromagnetic generator and six fan blades of 4 cm were employed as the wind energy harvester. The wind turbine was attached with the electronic circuit consisting of the autonomous sensor and the readout unit. Signals were transmitted through electromagnetic coupling at 125 kHz between the antenna of the transponder (U3280M) in the airflow-powered autonomous sensor and the transceiver (U2270B) in the readout unit. It was shown that the system was able to work at wind speeds higher than 4 m/s, with comparable wind speed predictions to the readings from a reference flowmeter, confirming the feasibility of powering autonomous sensors for airspeed monitoring with airflow energy.

In a subsequent study, Sardini and Serpelloni [164] extended the application of the integrated harvester and sensor to monitor the air temperature. A small-scale wind turbine consisting of a DC servomotor (1624T1, 4G9 Faulhaber) of $32 \times 32 \times 22$ mm and two blades of 65 mm diameter was attached with an autonomous sensing system consisting of a microcontroller, an integrated temperature sensor, and a radio-frequency transmitter. The system was able to transmit

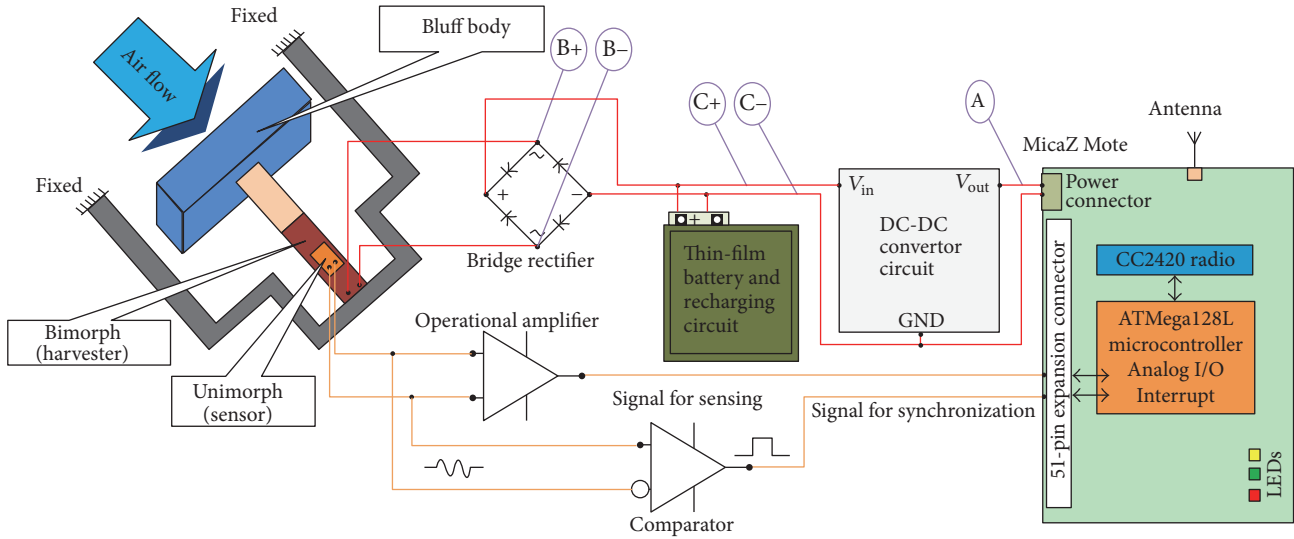


FIGURE 6: Schematic of Trinity indoor sensing system [34].

signal at wind speeds higher than 3 m/s with a 433-MHz point-to-point communication to a receiver placed within 4~5 m distance from the sensor with a time interval of 2 s. It was concluded that the self-powered wireless sensor harvesting ambient airflow energy can be applied in environmental health monitoring applications.

Along with the recently increasing desire on indoor microclimate control, Li et al. [34] developed the first documented Trinity system, that is, wind energy harvesting, synchronous duty-cycling, and sensing, as a self-sustaining sensing system to monitor and control the wind speed at individual outlets of a HVAC system according to real-time population density. The schematic of the Trinity is shown in Figure 6. The energy generated from a galloping-based energy harvester that consisted of a bimorph and a square sectioned bluff body was delivered to the power management module to power the sensor and charge the two thin-film batteries (if surplus energy was available). Low-power self-calibration strategy and per-link synchronization were implemented for synchronous duty-cycling to ensure the receivers to wake up in time to receive data packets from the respective senders. The low duty-cycles ($<0.42\%$) were due to the fact that the energy harvested was not sufficient to continuously activate the sensing nodes. The wind speed was inferred by sampling the voltage of the harvester based on the measured relationship between voltage and wind speed, accomplished with an amplifier circuit consuming a low power more than $500 \mu\text{W}$. The Trinity prototype successfully predicted agreed wind speeds with an anemometer within 3~6 m/s at 16 HVAC outlets. It was concluded that the Trinity is a successful demonstration of a self-powered indoor sensing system given a carefully designed network operation mode.

5. Conclusions

This paper reviews the state-of-the-art techniques of small-scale energy harvesting from a quantitative aspect.

Miniaturized windmills or wind turbines can generate a significant amount of power. Yet the biggest concern is that the rotary components are not desired for long-term use of such small sized devices. Besides the windmills and turbines, summaries of various devices based on VIV, galloping, flutter, wake galloping, TIV, and other types reviewed are presented in Tables 2–8. Their merits, limitations, applicabilities, and other information that the authors feel useful are also given in the tables. It should be noted that each technique investigated is suitable for a specific condition and has weakness in other conditions. One should choose a suitable technique or design according to the specific wind flow conditions, like whether the flow is smooth or turbulent, whether the flow speed is stable or frequently varies, and what the dominant wind speed range is, and so forth. As for the financial consideration, the cost of an energy harvester depends on various factors, such as the size, the transduction mechanism, and the type of piezoelectric material used. Typically, a single piece of commercial ready-to-mount piezoelectric sheet costs around \$50~80, such as the MFC sheet [165] and the DuraAct sheet [166]. Prices should go down for purchases in large volume. Also, raw piezoelectric sheets cost much less; for example, the PZT sheet without soldered wires costs less than $\$1/\text{cm}^2$ (Piezo Systems, Inc.), and the raw PVDF costs less than $\$1/\text{cm}^2$ [167]. For designs incorporating magnets, a $10 \text{ mm} \times 5 \text{ mm}$ neodymium magnet costs as low as $\$2$ [168], yet building a sophisticated rotor for a small turbine should inevitably cost much more. Increase in size of the harvester will usually cost more. Considering the ever-reduced power requirement of the wireless sensor, a harvester in cm scale is reasonably sufficient to power a sensor unit. Moreover, there are some commercial power management devices for convenient integration of energy harvesting module and sensor module, such as the LTC3330 chip [169] which costs $\$5$. With the fast technology development, it can be anticipated that a totally self-powered WSN can be built at a reasonable cost.

The authors hope to provide some useful guidance for researchers who are interested in small-scale wind energy harvesting and help them build a quantitative understanding. With future efforts in developing integrated self-powered electronics, like autonomous sensors incorporating wind energy harvesting and sensing techniques, the concept of wind energy harvesting will be finally led to real engineering applications.

Conflicts of Interest

The authors declare that they have no conflicts of interest regarding the publication of this paper.

References

- [1] S. Roundy, P. K. Wright, and J. Rabaey, "A study of low level vibrations as a power source for wireless sensor nodes," *Computer Communications*, vol. 26, no. 11, pp. 1131–1144, 2003.
- [2] P. D. Mitcheson, P. Miao, B. H. Stark, E. M. Yeatman, A. S. Holmes, and T. C. Green, "MEMS electrostatic micropower generator for low frequency operation," *Sensors and Actuators A: Physical*, vol. 115, no. 2-3, pp. 523–529, 2004.
- [3] M. El-Hami, P. Glynn-Jones, N. M. White et al., "Design and fabrication of a new vibration-based electromechanical power generator," *Sensors and Actuators, A: Physical*, vol. 92, no. 1-3, pp. 335–342, 2001.
- [4] S. P. Beeby, M. J. Tudor, and N. M. White, "Energy harvesting vibration sources for microsystems applications," *Measurement Science and Technology*, vol. 17, no. 12, article R01, pp. R175–R195, 2006.
- [5] S. R. Anton and H. A. Sodano, "A review of power harvesting using piezoelectric materials (2003–2006)," *Smart Materials and Structures*, vol. 16, no. 3, pp. R1–R21, 2007.
- [6] A. Erturk, *Electromechanical modeling of piezoelectric energy harvesters [Ph.D. thesis]*, Virginia Polytechnic Institute and State University, 2009.
- [7] L. Tang, Y. Yang, and C. K. Soh, "Toward broadband vibration-based energy harvesting," *Journal of Intelligent Material Systems and Structures*, vol. 21, no. 18, pp. 1867–1897, 2010.
- [8] M. A. Karami, *Micro-scale and nonlinear vibrational energy harvesting [Ph.D. thesis]*, Virginia Polytechnic Institute and State University, 2012.
- [9] Y. Wang, *Simultaneous energy harvesting and vibration control via piezoelectric materials [Ph.D. thesis]*, Virginia Polytechnic Institute and State University, 2012.
- [10] R. L. Harne and K. W. Wang, "A review of the recent research on vibration energy harvesting via bistable systems," *Smart Materials and Structures*, vol. 22, no. 2, Article ID 023001, 2013.
- [11] H. S. Kim, J.-H. Kim, and J. Kim, "A review of piezoelectric energy harvesting based on vibration," *International Journal of Precision Engineering and Manufacturing*, vol. 12, no. 6, pp. 1129–1141, 2011.
- [12] S. P. Pellegrini, N. Tolou, M. Schenk, and J. L. Herder, "Bistable vibration energy harvesters: a review," *Journal of Intelligent Material Systems and Structures*, vol. 24, no. 11, pp. 1303–1312, 2013.
- [13] M. F. Daqaq, R. Masana, A. Erturk, and D. D. Quinn, "On the role of nonlinearities in vibratory energy harvesting: a critical review and discussion," *Applied Mechanics Reviews*, vol. 66, no. 4, Article ID 040801, 2014.
- [14] H. D. Akaydin, *Piezoelectric energy harvesting from fluid flow [Ph.D. thesis]*, City University of New York, 2012.
- [15] A. Abdelkefi, *Global nonlinear analysis of piezoelectric energy harvesting from ambient and aeroelastic vibrations [Ph.D. thesis]*, Virginia Polytechnic Institute and State University, 2012.
- [16] M. Bryant, *Aeroelastic flutter vibration energy harvesting: modeling, testing, and system design [Ph.D. thesis]*, Cornell University, 2012.
- [17] J. D. Hobeck, *Energy harvesting with piezoelectric grass for autonomous self-sustaining sensor networks [Ph.D. thesis]*, The University of Michigan, 2014.
- [18] A. Bibo, *Investigation of concurrent energy harvesting from ambient vibrations and wind [Ph.D. thesis]*, Clemson University, 2014.
- [19] L. Zhao, *Small-scale wind energy harvesting using piezoelectric materials [Ph.D. thesis]*, Nanyang Technological University, 2015.
- [20] Q. Xiao and Q. Zhu, "A review on flow energy harvesters based on flapping foils," *Journal of Fluids and Structures*, vol. 46, pp. 174–191, 2014.
- [21] J. M. McCarthy, S. Watkins, A. Deivasigamani, and S. J. John, "Fluttering energy harvesters in the wind: a review," *Journal of Sound and Vibration*, vol. 361, pp. 355–377, 2016.
- [22] S. Priya, C.-T. Chen, D. Fye, and J. Zahnd, "Piezoelectric Windmill: a novel solution to remote sensing," *Japanese Journal of Applied Physics*, vol. 44, pp. L104–L107, 2005.
- [23] H. D. Akaydin, N. Elvin, and Y. Andreopoulos, "The performance of a self-excited fluidic energy harvester," *Smart Materials and Structures*, vol. 21, no. 2, Article ID 025007, 2012.
- [24] L. Zhao and Y. Yang, "Enhanced aeroelastic energy harvesting with a beam stiffener," *Smart Materials and Structures*, vol. 24, no. 3, Article ID 032001, 2015.
- [25] L. Zhao and Y. Yang, "Analytical solutions for galloping-based piezoelectric energy harvesters with various interfacing circuits," *Smart Materials and Structures*, vol. 24, no. 7, Article ID 075023, 2015.
- [26] M. Bryant and E. Garcia, "Modeling and testing of a novel aeroelastic flutter energy harvester," *Journal of Vibration and Acoustics*, vol. 133, no. 1, Article ID 011010, 2011.
- [27] H.-J. Jung and S.-W. Lee, "The experimental validation of a new energy harvesting system based on the wake galloping phenomenon," *Smart Materials and Structures*, vol. 20, no. 5, Article ID 055022, 2011.
- [28] J. D. Hobeck and D. J. Inman, "Artificial piezoelectric grass for energy harvesting from turbulence-induced vibration," *Smart Materials and Structures*, vol. 21, no. 10, Article ID 105024, 2012.
- [29] A. Truitt and S. N. Mahmoodi, "A review on active wind energy harvesting designs," *International Journal of Precision Engineering and Manufacturing*, vol. 14, no. 9, pp. 1667–1675, 2013.
- [30] J. Young, J. C. S. Lai, and M. F. Platzer, "A review of progress and challenges in flapping foil power generation," *Progress in Aerospace Sciences*, vol. 67, pp. 2–28, 2014.
- [31] A. Abdelkefi, "Aeroelastic energy harvesting: a review," *International Journal of Engineering Science*, vol. 100, pp. 112–135, 2016.
- [32] Y. Yang, L. Zhao, and L. Tang, "Comparative study of tip cross-sections for efficient galloping energy harvesting," *Applied Physics Letters*, vol. 102, no. 6, Article ID 064105, 2013.
- [33] L. Zhao, L. Tang, and Y. Yang, "Synchronized charge extraction in galloping piezoelectric energy harvesting," *Journal of Intelligent Material Systems and Structures*, vol. 27, no. 4, pp. 453–468, 2016.

- [34] F. Li, T. Xiang, Z. Chi et al., "Powering indoor sensing with airflows: a trinity of energy harvesting, synchronous duty-cycling, and sensing," in *Proceedings of the 11th ACM Conference on Embedded Networked Sensor Systems (SenSys '13)*, Roma, Italy, November 2013.
- [35] D. Rancourt, A. Tabesh, and L. G. Fr  chette, "Evaluation of centimeter-scale micro windmills: aerodynamics and electromagnetic power generation," in *Proceedings of the Power MEMS*, vol. 9, pp. 93–96, 2007.
- [36] D. A. Howey, A. Bansal, and A. S. Holmes, "Design and performance of a centimetre-scale shrouded wind turbine for energy harvesting," *Smart Materials and Structures*, vol. 20, no. 8, Article ID 085021, 2011.
- [37] S. Priya, "Modeling of electric energy harvesting using piezoelectric windmill," *Applied Physics Letters*, vol. 87, no. 18, Article ID 184101, 2005.
- [38] C.-T. Chen, R. A. Islam, and S. Priya, "Electric energy generator," *IEEE Transactions on Ultrasonics, Ferroelectrics, and Frequency Control*, vol. 53, no. 3, pp. 656–661, 2006.
- [39] R. Myers, M. Vickers, H. Kim, and S. Priya, "Small scale windmill," *Applied Physics Letters*, vol. 90, no. 5, Article ID 054106, 2007.
- [40] S. Bressers, D. Avirovik, M. Lallart, D. J. Inman, and S. Priya, "Contact-less wind turbine utilizing piezoelectric bimorphs with magnetic actuation," in *Proceedings of the 28th IMAC, A Conference on Structural Dynamics*, pp. 233–243, February 2010.
- [41] M. A. Karami, J. R. Farmer, and D. J. Inman, "Parametrically excited nonlinear piezoelectric compact wind turbine," *Renewable Energy*, vol. 50, pp. 977–987, 2013.
- [42] J. J. Allen and A. J. Smits, "Energy harvesting eel," *Journal of Fluids and Structures*, vol. 15, no. 3–4, pp. 629–640, 2001.
- [43] G. W. Taylor, J. R. Burns, S. M. Kammann, W. B. Powers, and T. R. Welsh, "The energy harvesting Eel: a small subsurface ocean/river power generator," *IEEE Journal of Oceanic Engineering*, vol. 26, no. 4, pp. 539–547, 2001.
- [44] W. P. Robbins, D. Morris, I. Marusic, and T. O. Novak, "Wind-generated electrical energy using flexible piezoelectric materials," in *Proceedings of the International Mechanical Engineering Congress and Exposition (ASME '06)*, pp. 581–590, Chicago, Ill, USA, November 2006.
- [45] S. Pobering and N. Schwesinger, "Power supply for wireless sensor systems," in *Proceedings of the 7th IEEE Conference on Sensors*, pp. 685–688, Lecce, Italy, October 2008.
- [46] S. Pobering, M. Menacher, S. Ebermaier, and N. Schwesinger, "Piezoelectric power conversion with self-induced oscillation," in *Proceedings of the PowerMEMS*, pp. 384–387, 2009.
- [47] H. D. Akaydin, N. Elvin, and Y. Andreopoulos, "Energy harvesting from highly unsteady fluid flows using piezoelectric materials," *Journal of Intelligent Material Systems and Structures*, vol. 21, no. 13, pp. 1263–1278, 2010.
- [48] H. D. Akaydin, N. Elvin, and Y. Andreopoulos, "Wake of a cylinder: a paradigm for energy harvesting with piezoelectric materials," *Experiments in Fluids*, vol. 49, no. 1, pp. 291–304, 2010.
- [49] L. A. Weinstein, M. R. Cacan, P. M. So, and P. K. Wright, "Vortex shedding induced energy harvesting from piezoelectric materials in heating, ventilation and air conditioning flows," *Smart Materials and Structures*, vol. 21, no. 4, Article ID 045003, 2012.
- [50] X. Gao, W.-H. Shih, and W. Y. Shih, "Flow energy harvesting using piezoelectric cantilevers with cylindrical extension," *IEEE Transactions on Industrial Electronics*, vol. 60, no. 3, pp. 1116–1118, 2013.
- [51] D.-A. Wang and H.-H. Ko, "Piezoelectric energy harvesting from flow-induced vibration," *Journal of Micromechanics and Microengineering*, vol. 20, no. 2, Article ID 025019, 2010.
- [52] D.-A. Wang, C.-Y. Chiu, and H.-T. Pham, "Electromagnetic energy harvesting from vibrations induced by K  rm  n vortex street," *Mechatronics*, vol. 22, no. 6, pp. 746–756, 2012.
- [53] H.-D. Tam Nguyen, H.-T. Pham, and D.-A. Wang, "A miniature pneumatic energy generator using K  rm  n vortex street," *Journal of Wind Engineering and Industrial Aerodynamics*, vol. 116, pp. 40–48, 2013.
- [54] J. Sirohi and R. Mahadik, "Piezoelectric wind energy harvester for low-power sensors," *Journal of Intelligent Material Systems and Structures*, vol. 22, no. 18, pp. 2215–2228, 2011.
- [55] J. Sirohi and R. Mahadik, "Harvesting wind energy using a galloping piezoelectric beam," *Journal of Vibration and Acoustics*, vol. 134, no. 1, Article ID 011009, 2012.
- [56] L. Zhao, L. Tang, and Y. Yang, "Small wind energy harvesting from galloping using piezoelectric materials," in *Proceedings of ASME 2012 Conference on Smart Materials, Adaptive Structures and Intelligent Systems (SMASIS '12)*, pp. 919–927, Nanjing, China, 2012.
- [57] L. Zhao, L. Tang, and Y. Yang, "Enhanced piezoelectric galloping energy harvesting using 2 degree-of-freedom cut-out cantilever with magnetic interaction," *Japanese Journal of Applied Physics*, vol. 53, no. 6, Article ID 060302, 2014.
- [58] L. Zhao, L. Tang, H. Wu, and Y. Yang, "Synchronized charge extraction for aeroelastic energy harvesting," in *Active and Passive Smart Structures and Integrated Systems*, vol. 9057 of *Proceedings of SPIE*, San Diego, Calif, USA, March 2014.
- [59] L. Zhao, J. Liang, L. Tang, Y. Yang, and H. Liu, "Enhancement of galloping-based wind energy harvesting by synchronized switching interface circuits," in *Proceedings of the SPIE Smart Structures and Materials, Nondestructive Evaluation and Health Monitoring*, vol. 9431, 2015.
- [60] L. Zhao, L. Tang, J. Liang, and Y. Yang, "Synergy of wind energy harvesting and synchronized switch harvesting interface circuit," *IEEE/ASME Transactions on Mechatronics*, vol. PP, no. 99, pp. 1–1, 2016.
- [61] A. Bibo, A. Abdelkefi, and M. F. Daqaq, "Modeling and characterization of a piezoelectric energy harvester under Combined Aerodynamic and Base Excitations," *ASME Journal of Vibration and Acoustics*, vol. 137, no. 3, Article ID 031017, 2015.
- [62] F. Ewere and G. Wang, "Performance of galloping piezoelectric energy harvesters," *Journal of Intelligent Material Systems and Structures*, vol. 25, no. 14, pp. 1693–1704, 2014.
- [63] M. Bryant and E. Garcia, "Energy harvesting: a key to wireless sensor nodes," in *Proceedings of the 2nd International Conference on Smart Materials and Nanotechnology in Engineering*, vol. 7493 of *Proceedings of SPIE*, Weihai, China, July 2009.
- [64] M. Bryant, R. Tse, and E. Garcia, "Investigation of host structure compliance in aeroelastic energy harvesting," in *Proceedings of the ASME Conference on Smart Materials, Adaptive Structures and Intelligent Systems*, pp. 769–775, 2012.
- [65] M. Bryant, M. Pizzonia, M. Mehallow, and E. Garcia, "Energy harvesting for self-powered aerostructure actuation," in *Proceedings of the Active and Passive Smart Structures and Integrated Systems 2014*, San Diego, Calif, USA, March 2014.
- [66] A. Erturk, W. G. R. Vieira, C. De Marqui Jr., and D. J. Inman, "On the energy harvesting potential of piezoaeroelastic systems," *Applied Physics Letters*, vol. 96, no. 18, Article ID 184103, 2010.

- [67] V. Sousa, M. de Anicézio, C. De Marqui Jr., and A. Erturk, "Enhanced aeroelastic energy harvesting by exploiting combined nonlinearities: theory and experiment," *Smart Materials and Structures*, vol. 20, no. 9, Article ID 094007, 2011.
- [68] A. Bibo and M. F. Daqaq, "Investigation of concurrent energy harvesting from ambient vibrations and wind using a single piezoelectric generator," *Applied Physics Letters*, vol. 102, no. 24, Article ID 243904, 2013.
- [69] S.-D. Kwon, "A T-shaped piezoelectric cantilever for fluid energy harvesting," *Applied Physics Letters*, vol. 97, no. 16, Article ID 164102, 2010.
- [70] J. Park, G. Morgenthal, K. Kim, S.-D. Kwon, and K. H. Law, "Power evaluation of flutter-based electromagnetic energy harvesters using computational fluid dynamics simulations," *Journal of Intelligent Material Systems and Structures*, vol. 25, no. 14, pp. 1800–1812, 2014.
- [71] S. Li, J. Yuan, and H. Lipson, "Ambient wind energy harvesting using cross-flow fluttering," *Journal of Applied Physics*, vol. 109, no. 2, Article ID 026104, 2011.
- [72] A. Deivasigamani, J. M. McCarthy, S. John, S. Watkins, P. Trivailo, and F. Coman, "Piezoelectric energy harvesting from wind using coupled bending-torsional vibrations," *Modern Applied Science*, vol. 8, no. 4, pp. 106–126, 2014.
- [73] J. D. Hobeck, D. Geslain, and D. J. Inman, "The dual cantilever flutter phenomenon: a novel energy harvesting method," in *Sensors and Smart Structures Technologies for Civil, Mechanical, and Aerospace Systems 2014*, vol. 9061 of *Proceedings of SPIE*, San Diego, Calif, USA, March 2014.
- [74] A. Abdelkefi, J. M. Scanlon, E. McDowell, and M. R. Hajj, "Performance enhancement of piezoelectric energy harvesters from wake galloping," *Applied Physics Letters*, vol. 103, no. 3, Article ID 033903, 2013.
- [75] A. Bibo, G. Li, and M. F. Daqaq, "Performance analysis of a harmonica-type aeroelastic micropower generator," *Journal of Intelligent Material Systems and Structures*, vol. 23, no. 13, pp. 1461–1474, 2012.
- [76] V. J. Ovejas and A. Cuadras, "Multimodal piezoelectric wind energy harvesters," *Smart Materials and Structures*, vol. 20, no. 8, Article ID 085030, 2011.
- [77] A. Bansal, D. A. Howey, and A. S. Holmes, "CM-scale air turbine and generator for energy harvesting from low-speed flows," in *Proceedings of the 15th International Conference on Solid-State Sensors, Actuators and Microsystems (TRANSDUCERS '09)*, pp. 529–532, Denver, Colo, USA, June 2009.
- [78] S. Bressers, C. Vernier, J. Regan et al., "Small-scale modular wind turbine," in *Active and Passive Smart Structures and Integrated Systems 2010*, vol. 7643 of *Proceedings of SPIE*, San Diego, Calif, USA, March 2010.
- [79] R. A. Kishore, T. Coudron, and S. Priya, "Small-scale wind energy portable turbine (SWEPT)," *Journal of Wind Engineering and Industrial Aerodynamics*, vol. 116, pp. 21–31, 2013.
- [80] L. Gu and C. Livermore, "Impact-driven, frequency up-converting coupled vibration energy harvesting device for low frequency operation," *Smart Materials and Structures*, vol. 20, no. 4, Article ID 045004, 2011.
- [81] A. Barrero-Gil, S. Pindado, and S. Avila, "Extracting energy from Vortex-Induced Vibrations: a parametric study," *Applied Mathematical Modelling*, vol. 36, no. 7, pp. 3153–3160, 2012.
- [82] A. Abdelkefi, M. R. Hajj, and A. H. Nayfeh, "Phenomena and modeling of piezoelectric energy harvesting from freely oscillating cylinders," *Nonlinear Dynamics*, vol. 70, no. 2, pp. 1377–1388, 2012.
- [83] A. Mehmood, A. Abdelkefi, M. R. Hajj, A. H. Nayfeh, I. Akhtar, and A. O. Nuhait, "Piezoelectric energy harvesting from vortex-induced vibrations of circular cylinder," *Journal of Sound and Vibration*, vol. 332, no. 19, pp. 4656–4667, 2013.
- [84] D.-A. Wang, H.-T. Pham, C.-W. Chao, and J. M. Chen, "A piezoelectric energy harvester based on pressure fluctuations in Kármán Vortex Street," in *Proceedings of the World Renewable Energy Congress*, Linköping, Sweden, May 2011.
- [85] O. Goushcha, N. Elvin, and Y. Andreopoulos, "Interactions of vortices with a flexible beam with applications in fluidic energy harvesting," *Applied Physics Letters*, vol. 104, no. 2, Article ID 021919, 2014.
- [86] J. Wang, J. Ran, and Z. Zhang, "Energy harvester based on the synchronization phenomenon of a circular cylinder," *Mathematical Problems in Engineering*, vol. 2014, Article ID 567357, 9 pages, 2014.
- [87] Vortex Bladeless Wind Generator, <http://www.vortexbladeless.com/>.
- [88] A. Barrero-Gil, G. Alonso, and A. Sanz-Andres, "Energy harvesting from transverse galloping," *Journal of Sound and Vibration*, vol. 329, no. 14, pp. 2873–2883, 2010.
- [89] F. Sorribes-Palmer and A. Sanz-Andres, "Optimization of energy extraction in transverse galloping," *Journal of Fluids and Structures*, vol. 43, pp. 124–144, 2013.
- [90] A. Abdelkefi, M. R. Hajj, and A. H. Nayfeh, "Power harvesting from transverse galloping of square cylinder," *Nonlinear Dynamics. An International Journal of Nonlinear Dynamics and Chaos in Engineering Systems*, vol. 70, no. 2, pp. 1355–1363, 2012.
- [91] A. Abdelkefi, Z. Yan, and M. R. Hajj, "Performance analysis of galloping-based piezoaeroelastic energy harvesters with different cross-section geometries," *Journal of Intelligent Material Systems and Structures*, vol. 25, no. 2, pp. 246–256, 2014.
- [92] L. Zhao, L. Tang, and Y. Yang, "Comparison of modeling methods and parametric study for a piezoelectric wind energy harvester," *Smart Materials and Structures*, vol. 22, no. 12, Article ID 125003, 2013.
- [93] A. Bibo and M. F. Daqaq, "On the optimal performance and universal design curves of galloping energy harvesters," *Applied Physics Letters*, vol. 104, no. 2, Article ID 023901, 2014.
- [94] A. Bibo and M. F. Daqaq, "An analytical framework for the design and comparative analysis of galloping energy harvesters under quasi-steady aerodynamics," *Smart Materials and Structures*, vol. 24, no. 9, Article ID 094006, 2015.
- [95] M. F. Daqaq, "Characterizing the response of galloping energy harvesters using actual wind statistics," *Journal of Sound and Vibration*, vol. 357, pp. 365–376, 2015.
- [96] F. Ewere, G. Wang, and B. Cain, "Experimental investigation of galloping piezoelectric energy harvesters with square bluff bodies," *Smart Materials and Structures*, vol. 23, no. 10, Article ID 104012, 2014.
- [97] D. Vicente-Ludlam, A. Barrero-Gil, and A. Velazquez, "Optimal electromagnetic energy extraction from transverse galloping," *Journal of Fluids and Structures*, vol. 51, pp. 281–291, 2014.
- [98] D. Vicente-Ludlam, A. Barrero-Gil, and A. Velazquez, "Enhanced mechanical energy extraction from transverse galloping using a dual mass system," *Journal of Sound and Vibration*, vol. 339, pp. 290–303, 2015.
- [99] L. Tang, M. P. Paidoussis, and J. Jiang, "Cantilevered flexible plates in axial flow: energy transfer and the concept of flutter-mill," *Journal of Sound and Vibration*, vol. 326, no. 1-2, pp. 263–276, 2009.

- [100] J. A. Dunnmon, S. C. Stanton, B. P. Mann, and E. H. Dowell, "Power extraction from aeroelastic limit cycle oscillations," *Journal of Fluids and Structures*, vol. 27, no. 8, pp. 1182–1198, 2011.
- [101] O. Doaré and S. Michelin, "Piezoelectric coupling in energy-harvesting fluttering flexible plates: linear stability analysis and conversion efficiency," *Journal of Fluids and Structures*, vol. 27, no. 8, pp. 1357–1375, 2011.
- [102] S. Michelin and O. Doaré, "Energy harvesting efficiency of piezoelectric flags in axial flows," *Journal of Fluid Mechanics*, vol. 714, pp. 489–504, 2013.
- [103] X. Shan, R. Song, Z. Xu, and T. Xie, "Dynamic energy harvesting performance of two Polyvinylidene Fluoride piezoelectric flags in parallel arrangement in an axial flow," in *Proceedings of the 15th International Conference on Electronic Packaging Technology (ICEPT '14)*, pp. 1–4, Chengdu, China, August 2014.
- [104] D. Zhao and E. Ega, "Energy harvesting from self-sustained aeroelastic limit cycle oscillations of rectangular wings," *Applied Physics Letters*, vol. 105, no. 10, Article ID 103903, 2014.
- [105] Y. H. Seo, B.-H. Kim, and D.-S. Choi, "Piezoelectric micro power harvester using flow-induced vibration for intrastructure health monitoring applications," *Microsystem Technologies*, vol. 21, no. 1, pp. 169–172, 2013.
- [106] C. De Marqui Jr., W. G. R. Vieira, A. Erturk, and D. J. Inman, "Modeling and analysis of piezoelectric energy harvesting from aeroelastic vibrations using the doublet-lattice method," *Journal of Vibration and Acoustics, Transactions of the ASME*, vol. 133, no. 1, Article ID 011003, 2011.
- [107] A. Abdelkefi, A. H. Nayfeh, and M. R. Hajj, "Design of piezoaeroelastic energy harvesters," *Nonlinear Dynamics*, vol. 68, no. 4, pp. 519–530, 2012.
- [108] Humdinger Wind Energy, Windbelt Innovation, http://www.humdingerwind.com/docs/IDDS_humdinger_techbrief_low-res.pdf.
- [109] Flutter mill, 2015 http://www.creative-science.org.uk/sharp_flutter.html.
- [110] P. Bade, "Flapping-vane wind machine," in *Proceedings of the International Conference of Appropriate Technologies for Semiarid Areas: Wind and Solar Energy for Water Supply*, pp. 83–88, 1976.
- [111] W. McKinney and J. DeLaurier, "Wingmill: an oscillating-wing windmill," *Journal of energy*, vol. 5, no. 2, pp. 109–115, 1981.
- [112] V. H. Schmidt, "Piezoelectric wind generator," Patent US4536674 A, 1985.
- [113] V. H. Schmidt, "Piezoelectric energy conversion in windmills," in *Proceedings of the IEEE Ultrasonics Symposium*, pp. 897–904, IEEE, 1992.
- [114] M. Bryant, E. Wolff, and E. Garcia, "Parametric design study of an aeroelastic flutter energy harvester," in *Proceedings of the SPIE Conference on Smart Structures and Materials: Active and Passive Smart Structures and Integrated Systems*, vol. 7977, San Diego, Calif, USA, March 2011.
- [115] M. Bryant, M. W. Shafer, and E. Garcia, "Power and efficiency analysis of a flapping wing wind energy harvester," in *Proceedings of the Active and Passive Smart Structures and Integrated Systems*, vol. 8341 of *Proceedings of SPIE*, San Diego, Calif, USA, March 2012.
- [116] M. Bryant, A. D. Schlichting, and E. Garcia, "Toward efficient aeroelastic energy harvesting: device performance comparisons and improvements through synchronized switching," in *Active and Passive Smart Structures and Integrated Systems*, vol. 8688 of *Proceedings of SPIE*, San Diego, Calif, USA, March 2013.
- [117] D. A. Peters, S. Karunamoorthy, and W.-M. Cao, "Finite state induced flow models part I: two-dimensional thin airfoil," *Journal of Aircraft*, vol. 32, no. 2, pp. 313–322, 1995.
- [118] A. Erturk, O. Bilgen, M. Fontenille, and D. J. Inman, "Piezoelectric energy harvesting from macro-fiber composites with an application to morphing-wing aircrafts," in *Proceedings of the 19th International Conference on Adaptive Structures and Technologies*, pp. 6–9, Ascona, Switzerland, 2008.
- [119] C. De Marqui and A. Erturk, "Electroaeroelastic analysis of airfoil-based wind energy harvesting using piezoelectric transduction and electromagnetic induction," *Journal of Intelligent Material Systems and Structures*, vol. 24, no. 7, pp. 846–854, 2013.
- [120] J. A. C. Dias, C. De Marqui Jr., and A. Erturk, "Hybrid piezoelectric-inductive flow energy harvesting and dimensionless electroaeroelastic analysis for scaling," *Applied Physics Letters*, vol. 102, no. 4, Article ID 044101, 2013.
- [121] J. A. C. Dias, C. De Marqui Jr., and A. Erturk, "Three-degree-of-freedom hybrid piezoelectric-inductive aeroelastic energy harvester exploiting a control surface," *AIAA Journal*, vol. 53, no. 2, pp. 394–404, 2015.
- [122] A. Abdelkefi, A. H. Nayfeh, and M. R. Hajj, "Modeling and analysis of piezoaeroelastic energy harvesters," *Nonlinear Dynamics. An International Journal of Nonlinear Dynamics and Chaos in Engineering Systems*, vol. 67, no. 2, pp. 925–939, 2012.
- [123] A. Bibo and M. F. Daqaq, "Energy harvesting under combined aerodynamic and base excitations," *Journal of Sound and Vibration*, vol. 332, no. 20, pp. 5086–5102, 2013.
- [124] J.-S. Bae and D. J. Inman, "Aeroelastic characteristics of linear and nonlinear piezo-aeroelastic energy harvester," *Journal of Intelligent Material Systems and Structures*, vol. 25, no. 4, pp. 401–416, 2014.
- [125] Y. Wu, D. Li, and J. Xiang, "Performance analysis and parametric design of an airfoil-based piezoaeroelastic energy harvester," in *Proceedings of the 56th AIAA/ASCE/AHS/ASC Structures, Structural Dynamics, and Materials Conference*, 13 pages, Kissimmee, Fla, USA, January 2015.
- [126] C. Boragno, R. Festa, and A. Mazzino, "Elastically bounded flapping wing for energy harvesting," *Applied Physics Letters*, vol. 100, no. 25, Article ID 253906, 2012.
- [127] S. Li and H. Lipson, "Vertical-stalk flapping-leaf generator for wind energy harvesting," in *Proceedings of the ASME Conference on Smart Materials, Adaptive Structures and Intelligent Systems (SMASIS '09)*, pp. 611–619, Oxnard, Calif, USA, September 2009.
- [128] J. M. McCarthy, A. Deivasigamani, S. J. John, S. Watkins, F. Coman, and P. Petersen, "Downstream flow structures of a fluttering piezoelectric energy harvester," *Experimental Thermal and Fluid Science*, vol. 51, pp. 279–290, 2013.
- [129] J. M. McCarthy, A. Deivasigamani, S. Watkins, S. J. John, F. Coman, and P. Petersen, "On the visualisation of flow structures downstream of fluttering piezoelectric energy harvesters in a tandem configuration," *Experimental Thermal and Fluid Science*, vol. 57, pp. 407–419, 2014.
- [130] C. De Marqui Jr., A. Erturk, and D. J. Inman, "Piezoaeroelastic modeling and analysis of a generator wing with continuous and segmented electrodes," *Journal of Intelligent Material Systems and Structures*, vol. 21, no. 10, pp. 983–993, 2010.
- [131] C. De Marqui Jr., A. Erturk, and D. J. Inman, "An electromechanical finite element model for piezoelectric energy harvester plates," *Journal of Sound and Vibration*, vol. 327, no. 1-2, pp. 9–25, 2009.
- [132] J. D. Hobeck and D. J. Inman, "A distributed parameter electromechanical and statistical model for energy harvesting from

- turbulence-induced vibration,” *Smart Materials and Structures*, vol. 23, no. 11, Article ID 115003, 2014.
- [133] N. G. Elvin and A. A. Elvin, “The flutter response of a piezoelectrically damped cantilever pipe,” *Journal of Intelligent Material Systems and Structures*, vol. 20, no. 16, pp. 2017–2026, 2009.
- [134] C. A. K. Kwuimy, G. Litak, M. Borowiec, and C. Nataraj, “Performance of a piezoelectric energy harvester driven by air flow,” *Applied Physics Letters*, vol. 100, no. 2, Article ID 024103, 2012.
- [135] S. P. Matova, R. Elfrink, R. J. M. Vullers, and R. Van Schaijk, “Harvesting energy from airflow with a micromachined piezoelectric harvester inside a Helmholtz resonator,” *Journal of Micromechanics and Microengineering*, vol. 21, no. 10, Article ID 104001, 2011.
- [136] S. Roundy, E. S. Leland, J. Baker et al., “Improving power output for vibration-based energy scavengers,” *IEEE Pervasive Computing*, vol. 4, no. 1, pp. 28–36, 2005.
- [137] M. Arafa, W. Akl, A. Aladwani, O. Aldraihem, and A. Baz, “Experimental implementation of a cantilevered piezoelectric energy harvester with a dynamic magnifier,” in *Proceedings of the Active and Passive Smart Structures and Integrated Systems*, vol. 7977 of *Proceedings of SPIE*, San Diego, Calif, USA, March 2011.
- [138] H. Wu, L. Tang, Y. Yang, and C. K. Soh, “A compact 2 degree-of-freedom energy harvester with cut-out cantilever beam,” *Japanese Journal of Applied Physics*, vol. 51, no. 4, Article ID 040211, 2012.
- [139] J. E. Kim and Y. Y. Kim, “Power enhancing by reversing mode sequence in tuned mass-spring unit attached vibration energy harvester,” *AIP Advances*, vol. 3, no. 7, Article ID 072103, 2013.
- [140] A. M. Wickenheiser and E. Garcia, “Broadband vibration-based energy harvesting improvement through frequency up-conversion by magnetic excitation,” *Smart Materials and Structures*, vol. 19, no. 6, Article ID 065020, 2010.
- [141] H. L. Dai, A. Abdelkefi, and L. Wang, “Modeling and nonlinear dynamics of fluid-conveying risers under hybrid excitations,” *International Journal of Engineering Science*, vol. 81, pp. 1–14, 2014.
- [142] H. L. Dai, A. Abdelkefi, and L. Wang, “Piezoelectric energy harvesting from concurrent vortex-induced vibrations and base excitations,” *Nonlinear Dynamics*, vol. 77, no. 3, pp. 967–981, 2014.
- [143] Z. Yan, A. Abdelkefi, and M. R. Hajj, “Piezoelectric energy harvesting from hybrid vibrations,” *Smart Materials and Structures*, vol. 23, no. 2, Article ID 025026, 2014.
- [144] F. Cottone, H. Vocca, and L. Gammaitoni, “Nonlinear energy harvesting,” *Physical Review Letters*, vol. 102, no. 8, Article ID 080601, 2009.
- [145] A. Erturk and D. J. Inman, “Broadband piezoelectric power generation on high-energy orbits of the bistable Duffing oscillator with electromechanical coupling,” *Journal of Sound and Vibration*, vol. 330, no. 10, pp. 2339–2353, 2011.
- [146] S. Zhou, J. Cao, A. Erturk, and J. Lin, “Enhanced broadband piezoelectric energy harvesting using rotatable magnets,” *Applied Physics Letters*, vol. 102, no. 17, Article ID 173901, 2013.
- [147] S. Zhou, J. Cao, D. J. Inman, J. Lin, S. Liu, and Z. Wang, “Broadband tristable energy harvester: modeling and experiment verification,” *Applied Energy*, vol. 133, pp. 33–39, 2014.
- [148] A. Bibo, A. H. Alhadidi, and M. F. Daqaq, “Exploiting a nonlinear restoring force to improve the performance of flow energy harvesters,” *Journal of Applied Physics*, vol. 117, no. 4, Article ID 045103, 2015.
- [149] G. K. Ottman, H. F. Hofmann, A. C. Bhatt, and G. A. Lesieutre, “Adaptive piezoelectric energy harvesting circuit for wireless remote power supply,” *IEEE Transactions on Power Electronics*, vol. 17, no. 5, pp. 669–676, 2002.
- [150] G. K. Ottman, H. F. Hofmann, and G. A. Lesieutre, “Optimized piezoelectric energy harvesting circuit using step-down converter in discontinuous conduction mode,” *IEEE Transactions on Power Electronics*, vol. 18, no. 2, pp. 696–703, 2003.
- [151] D. Guyomar, A. Badel, E. Lefeuvre, and C. Richard, “Toward energy harvesting using active materials and conversion improvement by nonlinear processing,” *IEEE Transactions on Ultrasonics, Ferroelectrics, and Frequency Control*, vol. 52, no. 4, pp. 584–594, 2005.
- [152] M. Lallart and D. Guyomar, “An optimized self-powered switching circuit for non-linear energy harvesting with low voltage output,” *Smart Materials and Structures*, vol. 17, no. 3, Article ID 035030, 2008.
- [153] Y. C. Shu, I. C. Lien, and W. J. Wu, “An improved analysis of the SSHI interface in piezoelectric energy harvesting,” *Smart Materials and Structures*, vol. 16, no. 6, pp. 2253–2264, 2007.
- [154] I. C. Lien, Y. C. Shu, W. J. Wu, S. M. Shiu, and H. C. Lin, “Revisit of series-SSHI with comparisons to other interfacing circuits in piezoelectric energy harvesting,” *Smart Materials and Structures*, vol. 19, no. 12, Article ID 125009, 2010.
- [155] E. Lefeuvre, A. Badel, C. Richard, L. Petit, and D. Guyomar, “A comparison between several vibration-powered piezoelectric generators for standalone systems,” *Sensors and Actuators, A: Physical*, vol. 126, no. 2, pp. 405–416, 2006.
- [156] J. Liang and W.-H. Liao, “An improved self-powered switching interface for piezoelectric energy harvesting,” in *Proceedings of the IEEE International Conference on Information and Automation (ICIA ’09)*, pp. 945–950, Zhuhai, China, June 2009.
- [157] J. Liang and W.-H. Liao, “Improved design and analysis of self-powered synchronized switch interface circuit for piezoelectric energy harvesting systems,” *IEEE Transactions on Industrial Electronics*, vol. 59, no. 4, pp. 1950–1960, 2012.
- [158] E. Lefeuvre, A. Badel, C. Richard, and D. Guyomar, “Piezoelectric energy harvesting device optimization by synchronous electric charge extraction,” *Journal of Intelligent Material Systems and Structures*, vol. 16, no. 10, pp. 865–876, 2005.
- [159] E. Lefeuvre, A. Badel, C. Richard, and D. Guyomar, “Energy harvesting using piezoelectric materials: case of random vibrations,” *Journal of Electroceramics*, vol. 19, no. 4, pp. 349–355, 2007.
- [160] L. Tang and Y. Yang, “Analysis of synchronized charge extraction for piezoelectric energy harvesting,” *Smart Materials and Structures*, vol. 20, no. 8, Article ID 085022, 2011.
- [161] A. M. Wickenheiser, T. Reissman, W.-J. Wu, and E. Garcia, “Modeling the effects of electromechanical coupling on energy storage through piezoelectric energy harvesting,” *IEEE/ASME Transactions on Mechatronics*, vol. 15, no. 3, pp. 400–411, 2010.
- [162] W. J. Wu, A. M. Wickenheiser, T. Reissman, and E. Garcia, “Modeling and experimental verification of synchronized discharging techniques for boosting power harvesting from piezoelectric transducers,” *Smart Materials and Structures*, vol. 18, no. 5, Article ID 055012, 2009.

- [163] A. Flammini, D. Marioli, E. Sardini, and M. Serpelloni, "An autonomous sensor with energy harvesting capability for air-flow speed measurements," in *Proceedings of the Instrumentation and Measurement Technology Conference (I2MTC '10)*, pp. 892–897, IEEE, Austin, Tex, USA, May 2010.
- [164] E. Sardini and M. Serpelloni, "Self-powered wireless sensor for air temperature and velocity measurements with energy harvesting capability," *IEEE Transactions on Instrumentation and Measurement*, vol. 60, no. 5, pp. 1838–1844, 2011.
- [165] Smart Material Corp, <http://www.smart-material.com/MFC-product-main.html>.
- [166] Physik Instrumente GmbH & Co. KG, <https://www.pic ceramic.com/en/products/piezoceramic-actuators/patch-transducers>.
- [167] Professional Plastics, Inc, <http://www.professionalplastics.com/PVDFFILM>.
- [168] Eclipse Magnetics Ltd, <http://www.professionalplastics.com/PVDFFILM>, <http://www.newark.com/eclipse-magnetics/n813/neodymium-disc-magnets-10mm-x/dp/74R0104>.
- [169] Linear Technology Corp, 2016 <http://www.linear.com/product/LTC3330>.

